united nations
educational, scientific
and cultural
organization

international atomic
energy agency

the
abdus salam
international centre for theoretical physics

SMR.1303 - 1

Advanced Course:
CLIMATE CHANGE IN THE MEDITERRANEAN REGION
PART I: PHYSICAL ASPECTS
(12 - 16 March 2001)

"Physical Principles of Climate Change"

Hervé LE TREUT
Laboratoire de Meteorologie Dynamique du CNRS
Jussieu, CNRS/UPMC
Boite 99
75252 Paris cedex 05
FRANCE

Climate sensitivity:
the physical processes

- Definitions, stability of climate equilibrium
  - → application to past climates
- Cloud and water vapour feedbacks
  - → model validation
- Transitions in the climate system: the role of the slow components

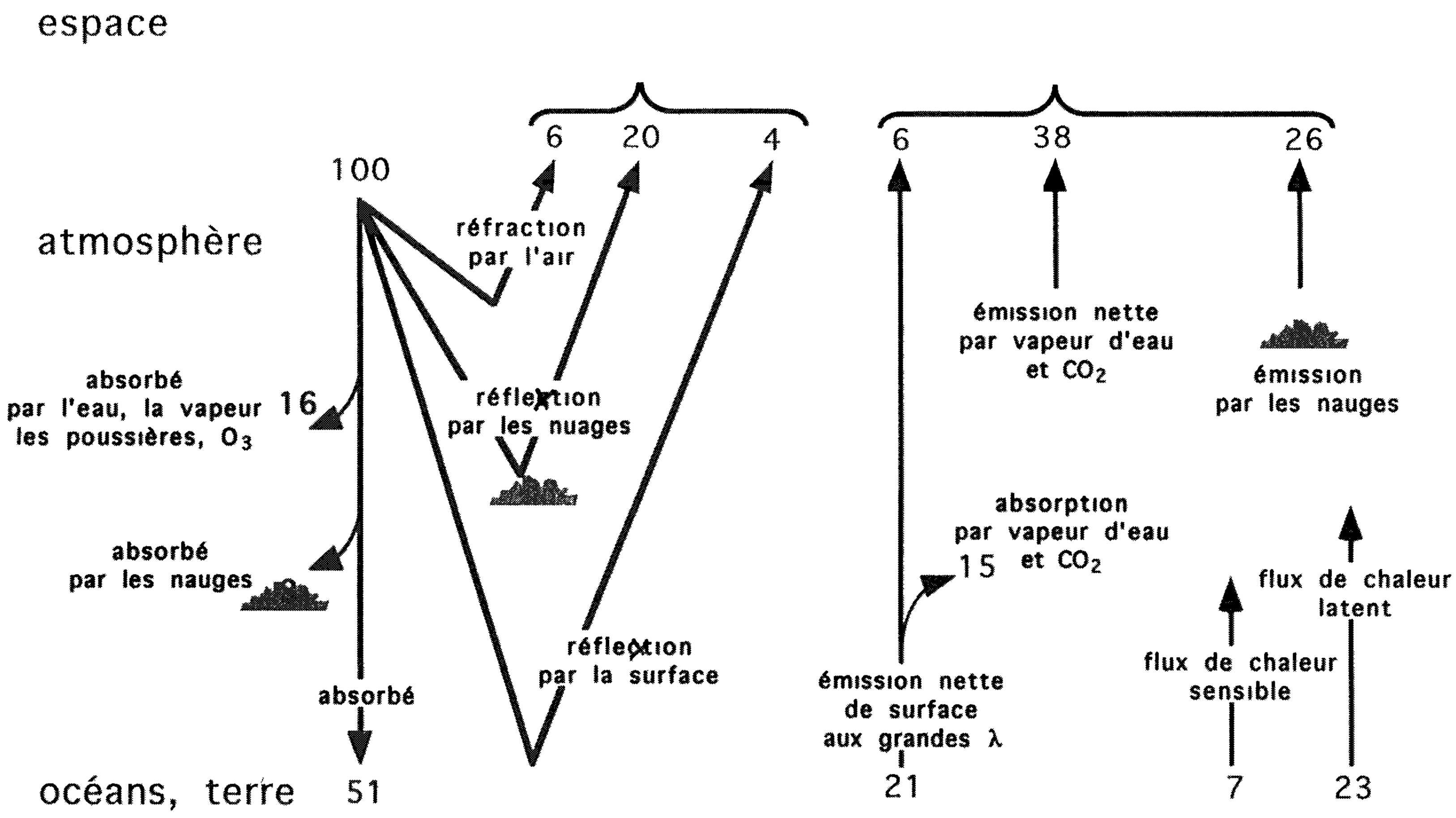

bilan radiatif moyen et flux de chaleur dans l'atmosphère
Les valeurs sont relatives à un flux solaire entrant de 100 unités

0-D approach of climate equilibrium

$$C \frac{dT}{dt} = \frac{S}{4}(1-\alpha) - OLR$$

$C \simeq$ heat capacity/surface unit

$T \simeq$ Sea Surface Temperature

We define g = greenhouse factor = $\dfrac{\sigma T^4 - OLR}{\sigma T^4}$

$$C \frac{dT}{dt} = B = \frac{S}{4}(1-\alpha) - \sigma T^4 (1-g)$$

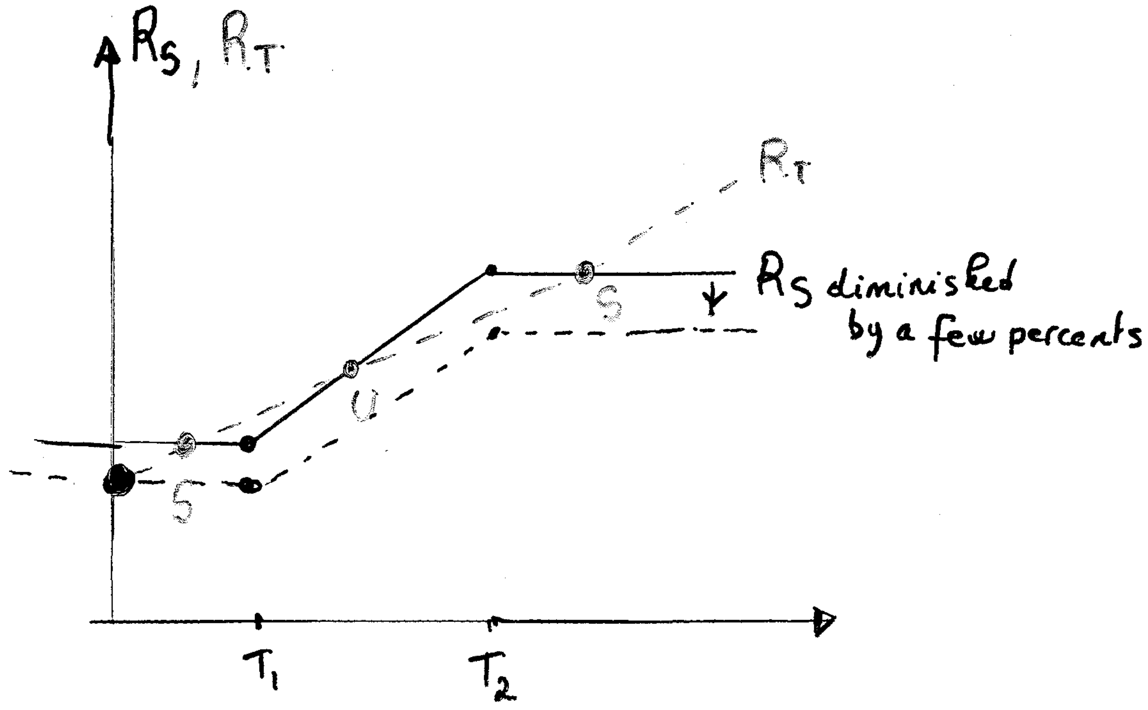
R_S, R_T
R_T
R_S diminished
by a few percents
S
U
S
T_1
T_2

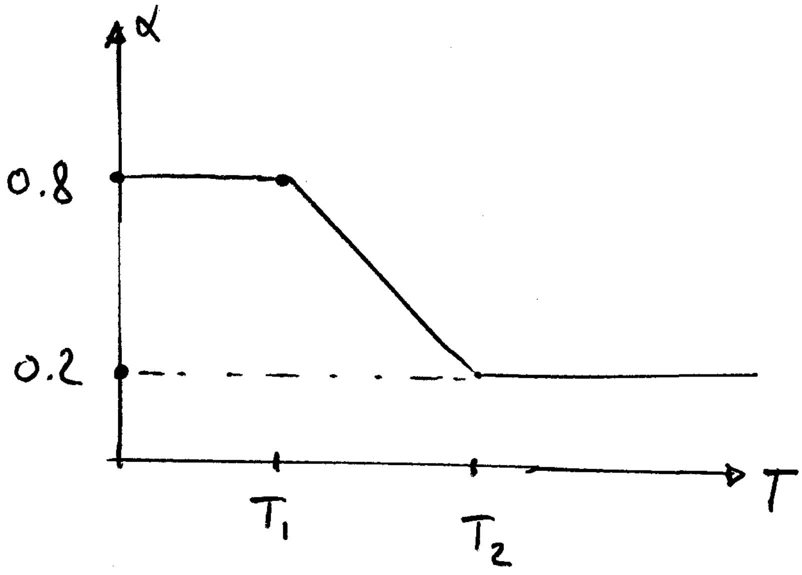
α
0.8
0.2
T_1
T_2
T

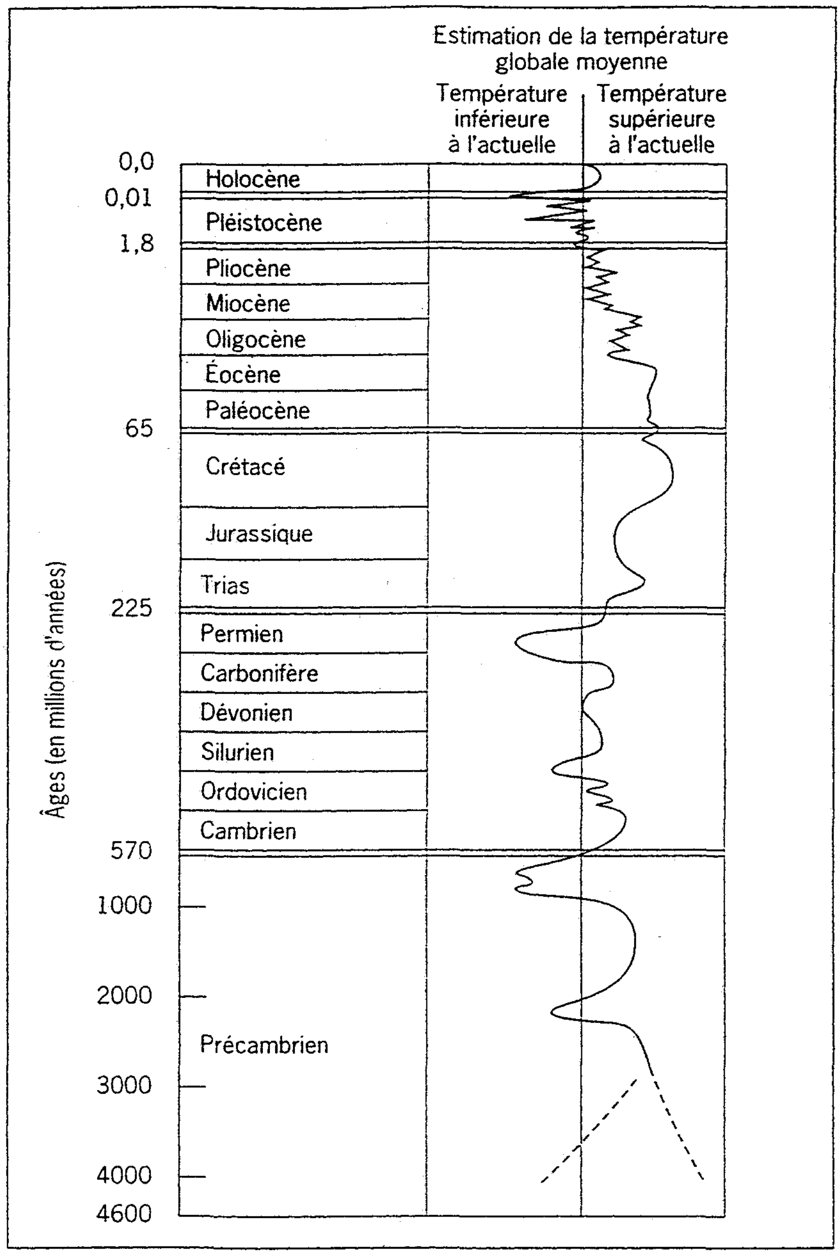

Différents indicateurs géologiques permettent de retracer l'allure générale de la courbe des changements de température de la Terre depuis son origine, il y a 4,6 milliards d'années. Ils mettent en évidence un climat généralement plus chaud que celui des deux derniers millions d'années.

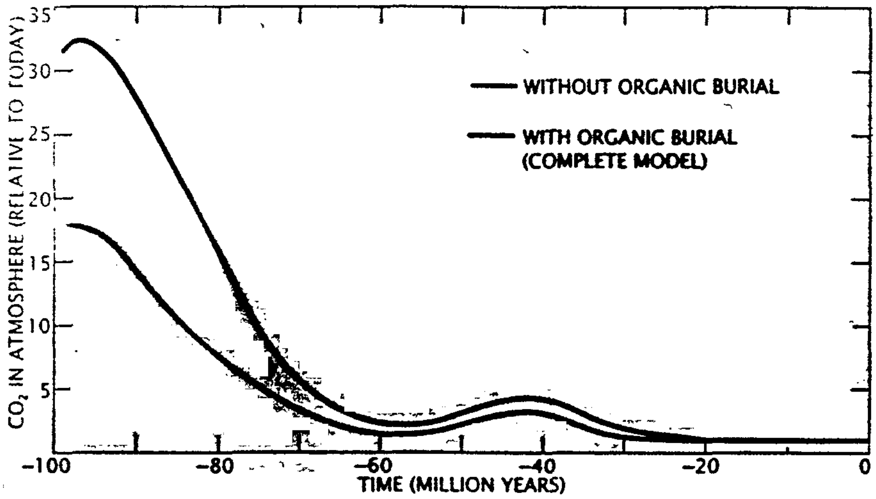

CARBON DIOXIDE content of the atmosphere relative to today's level is plotted for the past 100 million years, with a given set of parameters. The abundance of CO_2 is affected by the deposition and burial of organic matter (the soft carbon-bearing remains of plants and animals) in ancient swamps and sea floors. Such burial effectively removes CO_2 from the atmosphere, a fact reflected in the curves: the lower curve includes organic burial and results in less atmospheric CO_2, whereas the upper one is a model without organic burial, resulting in more atmospheric CO_2. The hump at about 40 million years ago reflects an increase in the rate of sea-floor spreading, leading to an increased degassing and atmospheric abundance of CO_2.

[redacted]

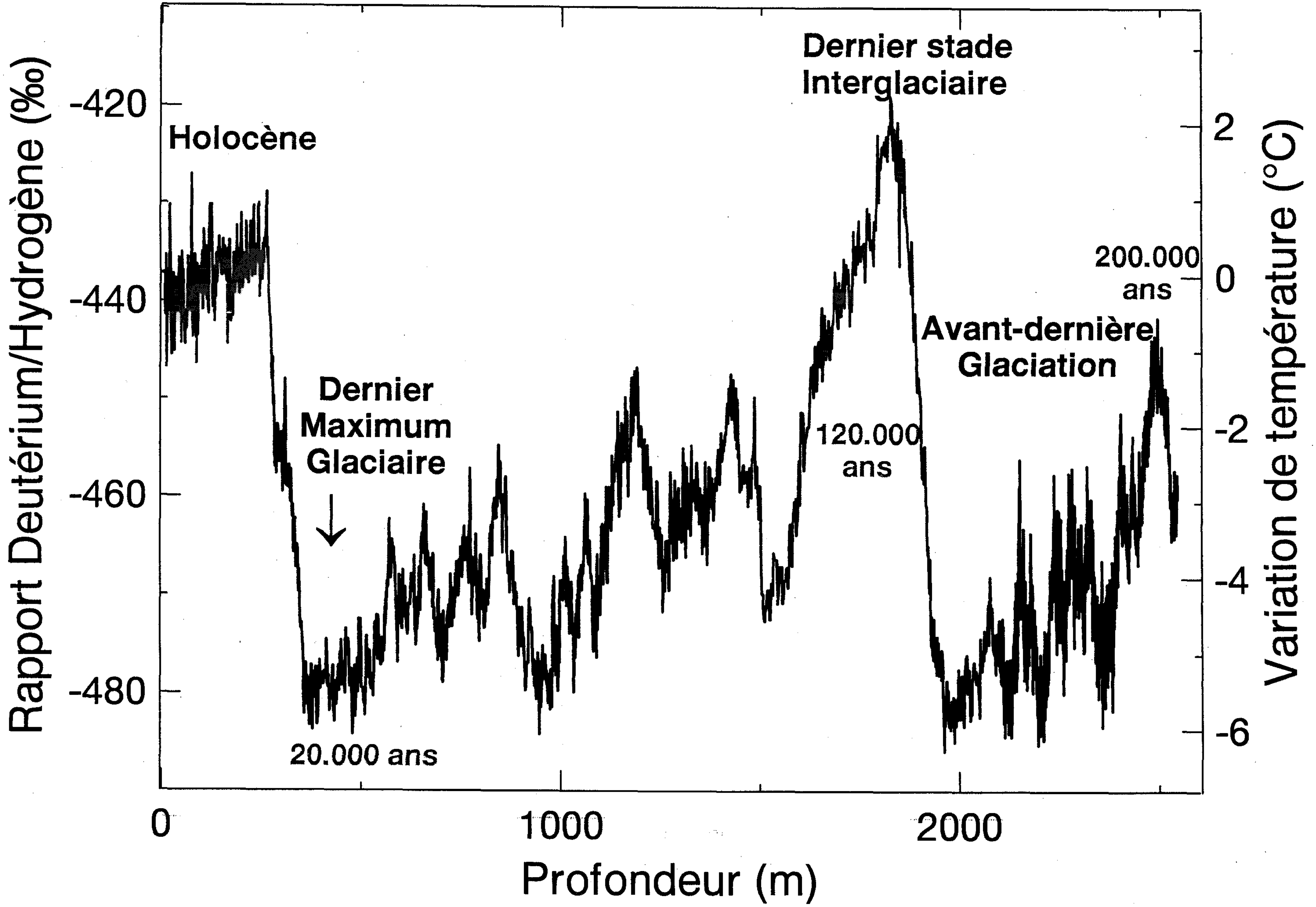
Rapport Deutérium/Hydrogène (‰)
-420
-440
-460
-480
Holocène
Dernier Maximum Glaciaire
20.000 ans
Dernier stade Interglaciaire
120.000 ans
Avant-dernière Glaciation
200.000 ans
0
1000
2000
Profondeur (m)
Variation de température (°C)
2
0
-2
-4
-6

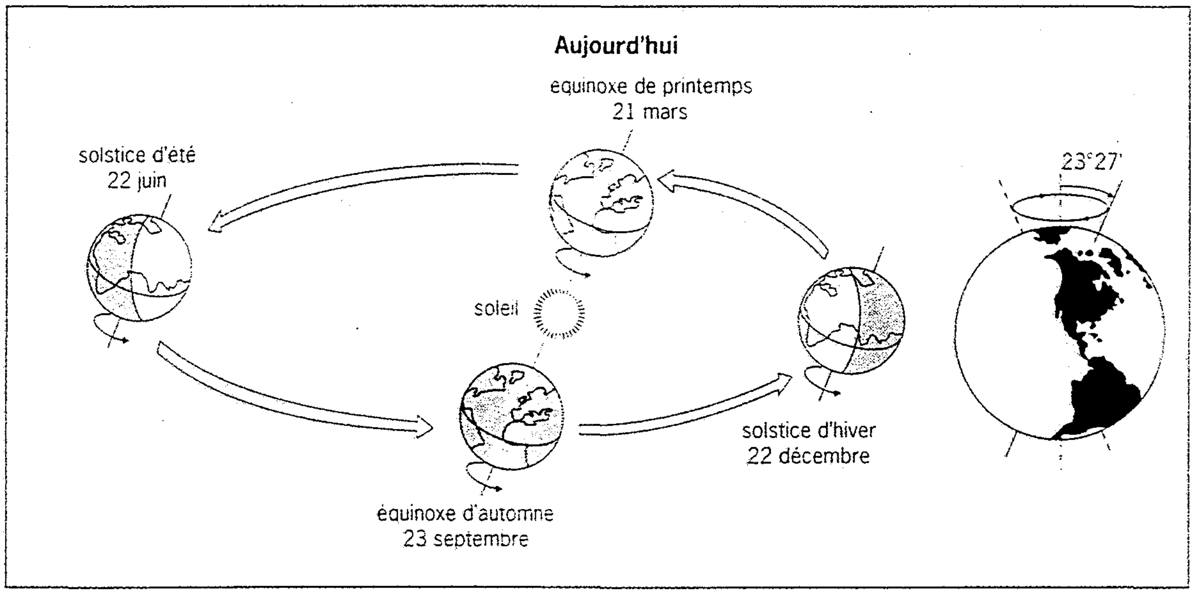
Aujourd'hui
équinoxe de printemps
21 mars
solstice d'été
22 juin
23°27'
soleil
solstice d'hiver
22 décembre
équinoxe d'automne
23 septembre

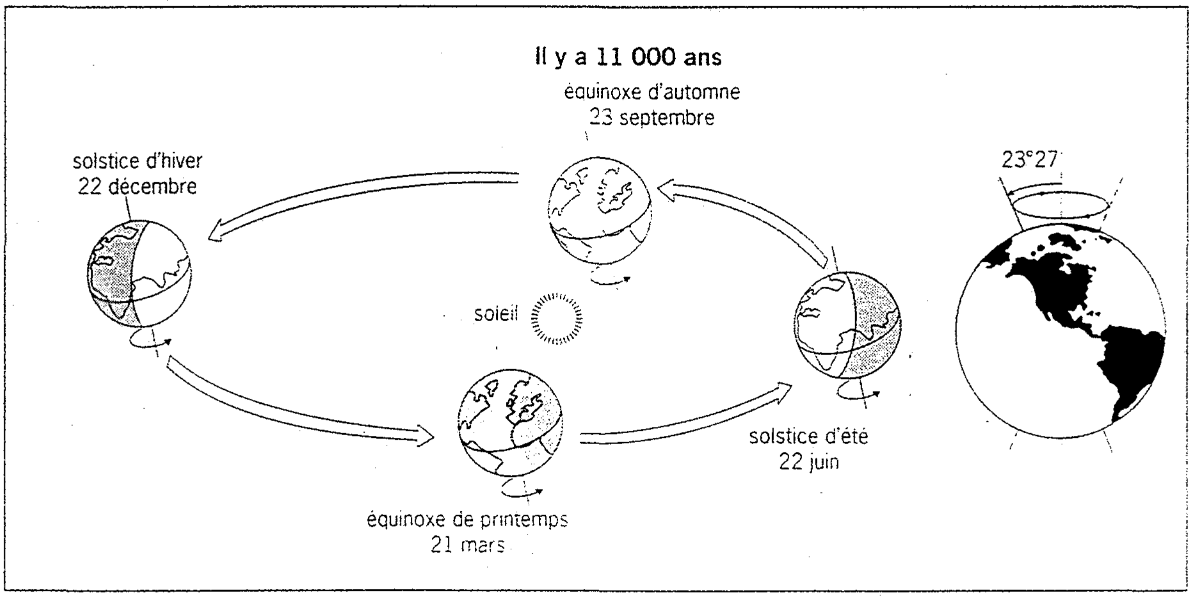
Il y a 11 000 ans
équinoxe d'automne
23 septembre
solstice d'hiver
22 décembre
23°27'
soleil
solstice d'été
22 juin
équinoxe de printemps
21 mars

EFFET DE LA PRECESSION

Difference de temperature au sol DJF [Celsius], (1.12-30.02)

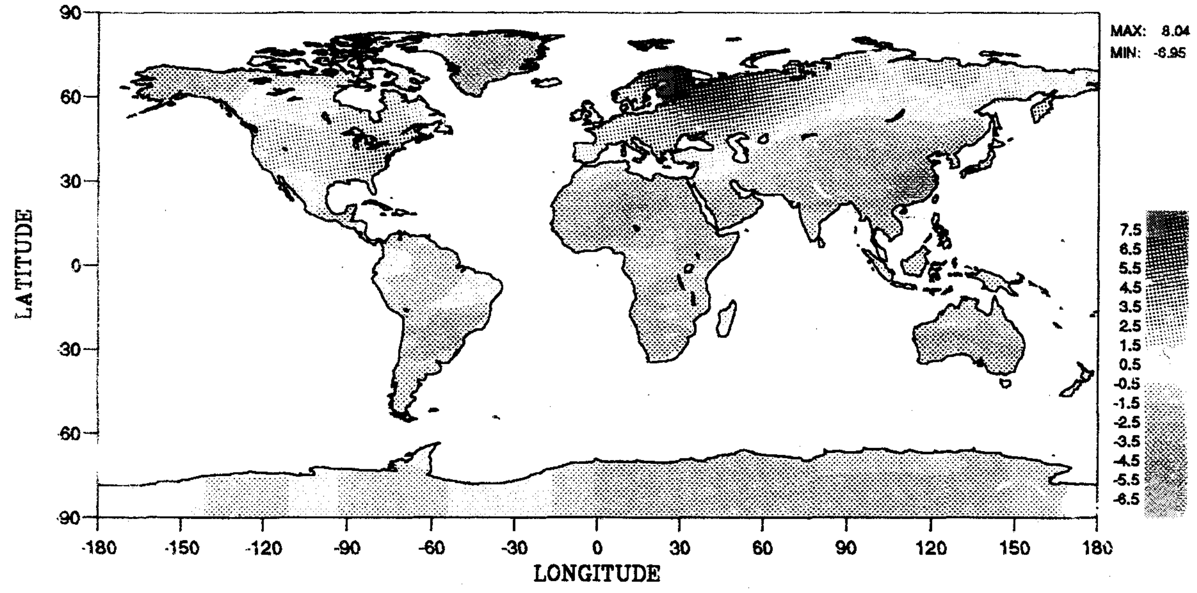

EFFET DE LA PRECESSION

Difference de temperature au sol JJA [Celsius], (01.06-30.08)

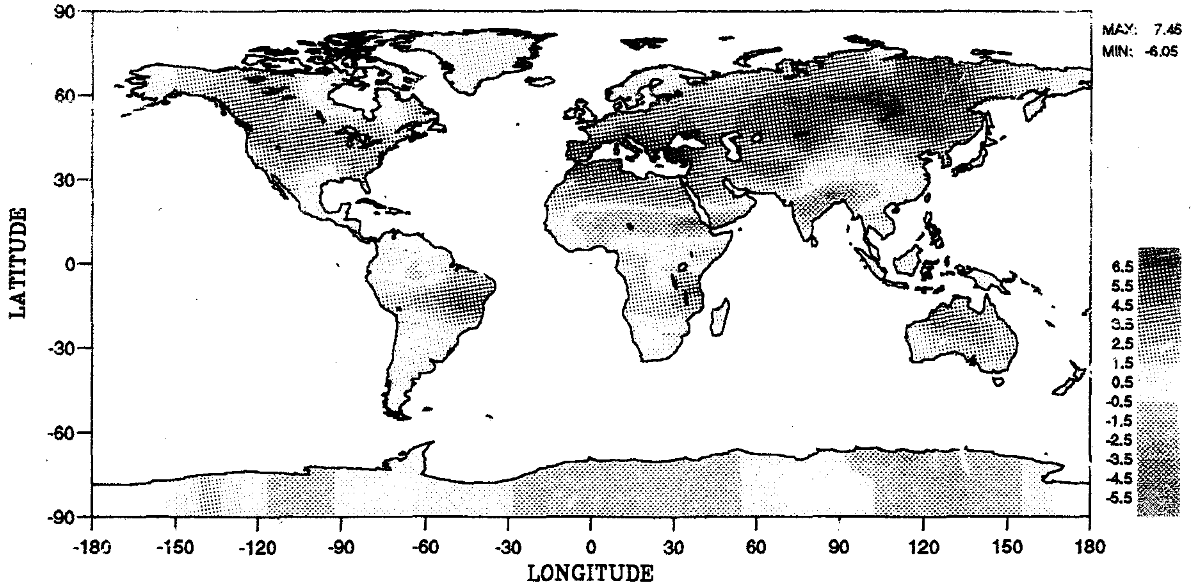

Equilibrium of the Tropics

(Pierrehumbert, 94) (JAS)
(Ide et al, 2001) (Climate Dynamics)

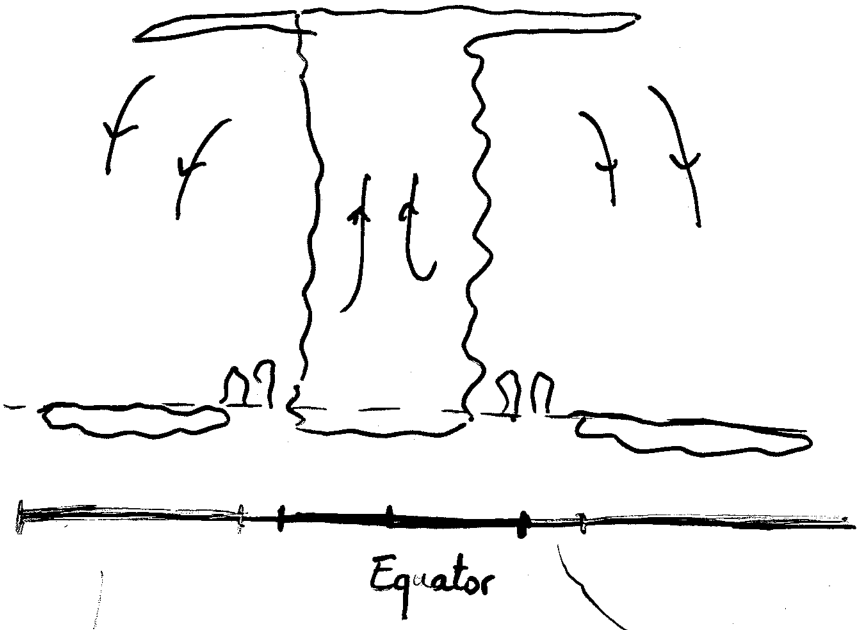

Subtropical areas: $T_{cloud} \simeq T_{soil}$

$$c \cdot \frac{dT}{dt} = \frac{S}{4} \cdot (1-\alpha) - \sigma \cdot T_{cloud}^4$$

stable

Equatorial areas:

- runaway WV greenhouse effect
- clouds? (thermostat?)

?

Feedbacks + Energy transport redistubute climate change over the globe

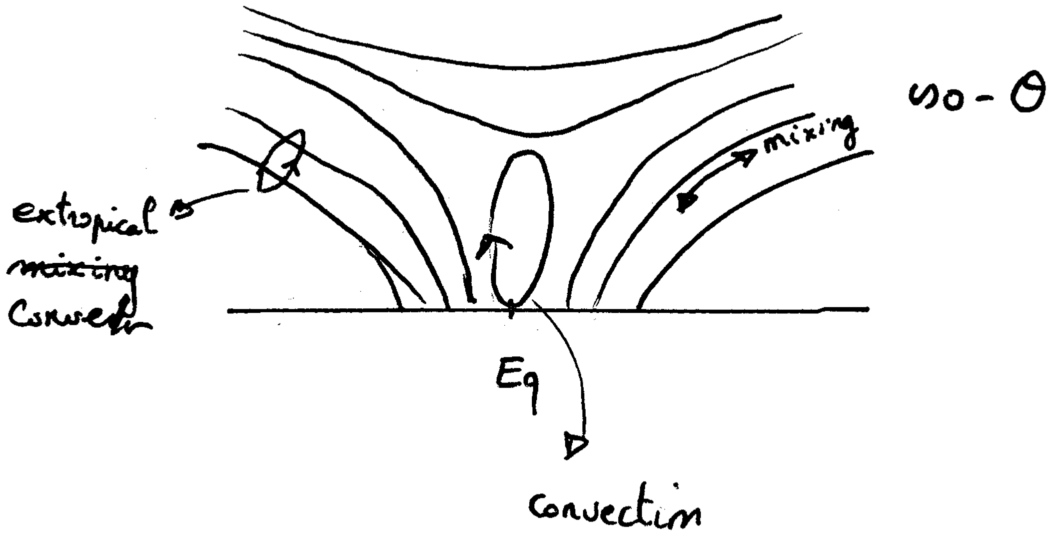

* Perturbations radiatives depuis le début de l'ère industrielle

(a) CO_2 forcing

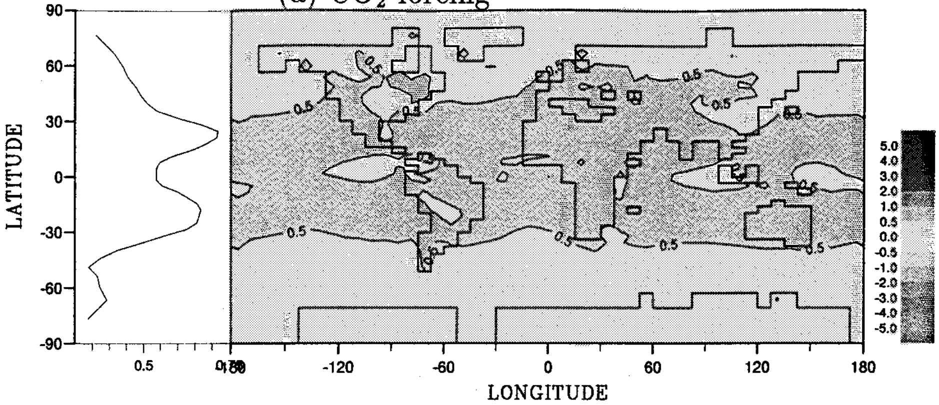

← CO_2

(b) Aerosol direct forcing

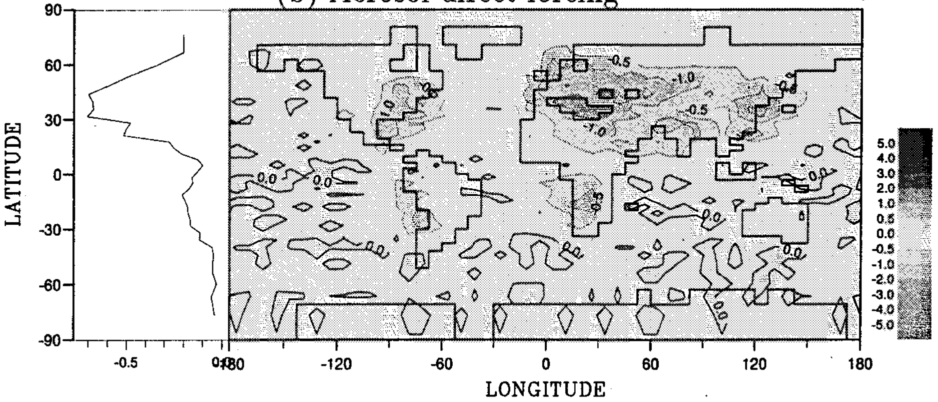

← Sulfates

(c) Aerosol indirect forcing

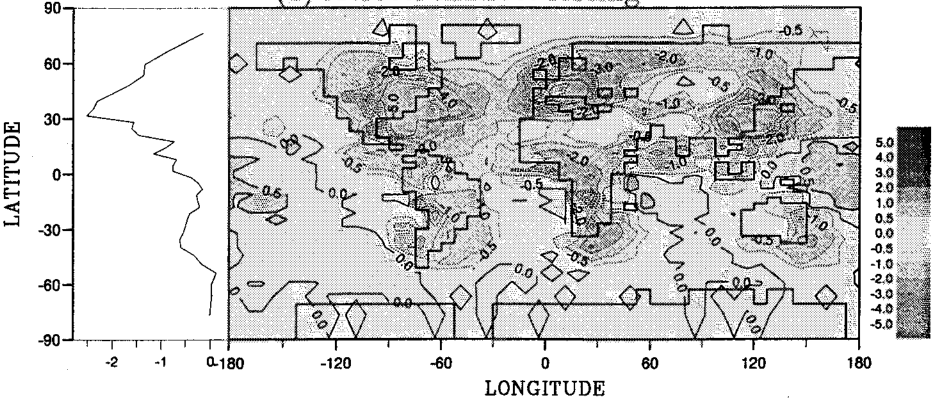

Figure 1: Climate forcings (Wm^{-2}) due to (a) the CO_2 greenhouse effect, (b) the aerosol direct effect, and (c) the aerosol indirect effect.

Mean change CONT-AERTOT in surface temperature [Celsius]

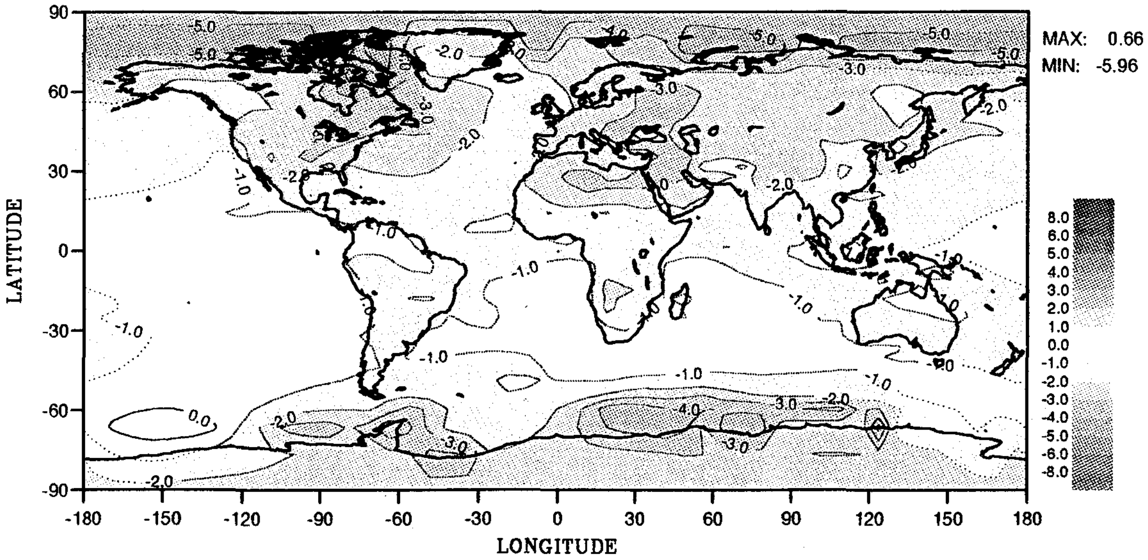

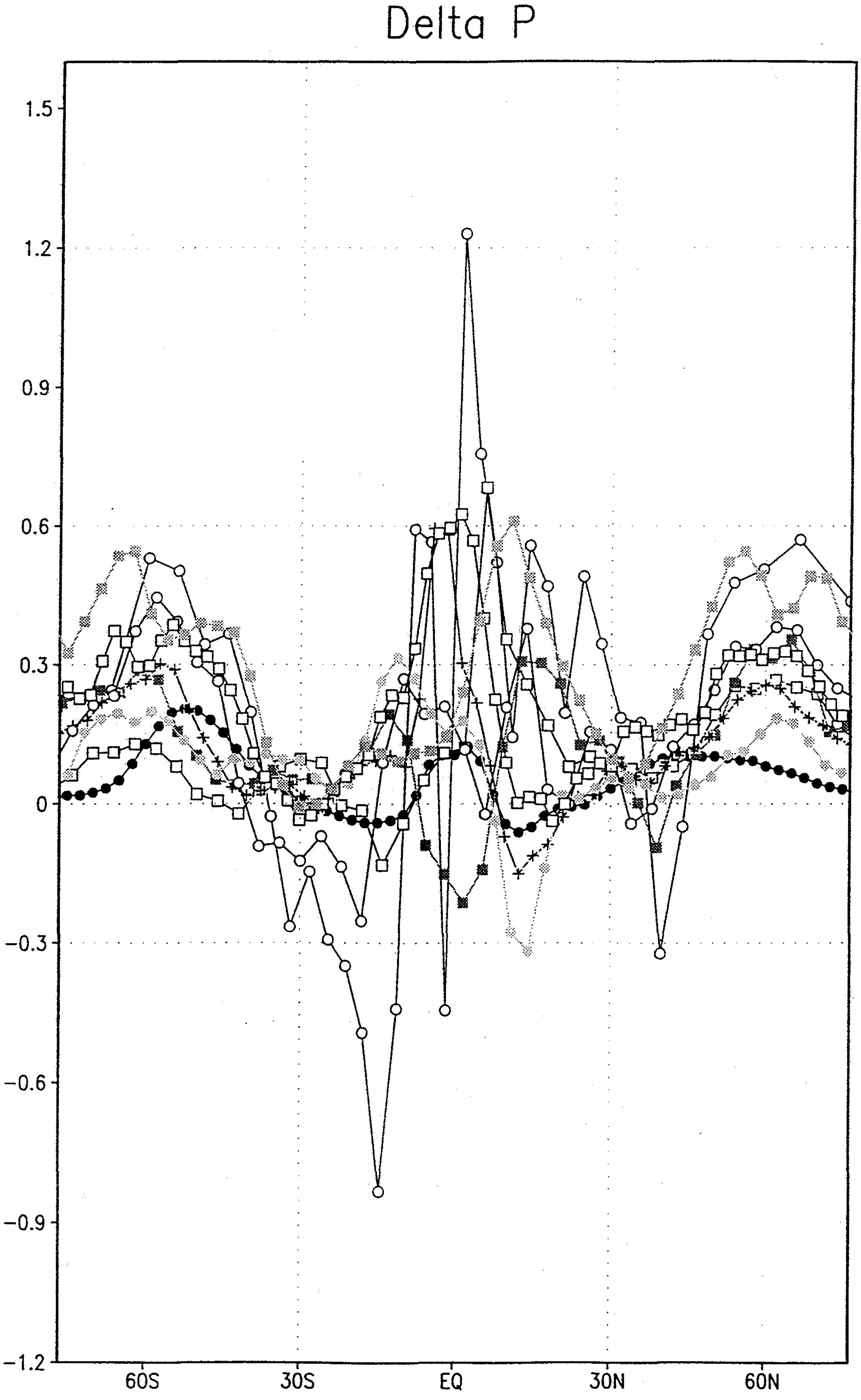
Delta P
1.5
1.2
0.9
0.6
0.3
0
−0.3
−0.6
−0.9
−1.2
60S
30S
EQ
30N
60N

MODIFICATIONS DE LA PLUVIOSITE POUR UN CLIMAT CHAUD

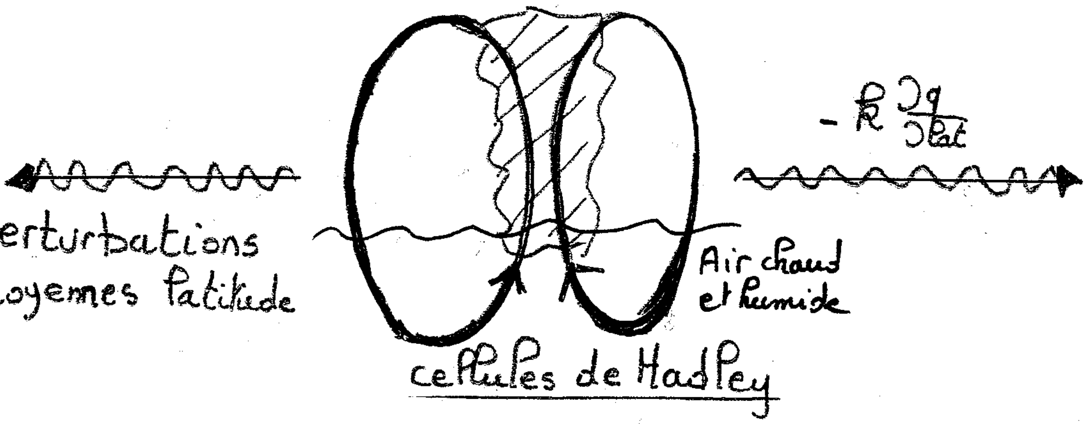

① Régions Tropicales:

Ralentissment de la cellule de Hadley
Augmentation de l'humidité et de la chaleur dans les couches
surface

② Régions de moyennes latitudes

Transport d'humidite = - k h $\left(\frac{\partial q_s}{\partial T}\right)\left(\frac{\partial T}{\partial lat}\right)$

k → diminue

h → ?

$\frac{\partial q_s}{\partial T}$ → augmente (et domine la réponse)

$\frac{\partial T}{\partial lat}$ → diminue

$$B = 0 = B(\underbrace{\lambda}_{\substack{\text{forcing}\\ \text{parameter}}}, T, \underbrace{q_i}_{\substack{\text{feedback parameters}\\ [\alpha,\ g \text{ or cloud, water vapour} \ldots]}})$$

$$\Delta T = \frac{\left.\frac{\partial B}{\partial \lambda}\right|_{T,q_i} \Delta\lambda \quad \leftarrow \text{forcing}}{\underbrace{\left[-\left.\frac{\partial B}{\partial T}\right|_{\lambda,q_i}\right]}_{\text{sensitivity}} \left[1 + \underbrace{\frac{\left.\frac{\partial B}{\partial q_i}\right|_{\lambda,T} \frac{\partial q}{\partial T}}{\left.\frac{\partial B}{\partial T}\right|_{\lambda,q_i}}}_{\text{feedbacks}}\right]}$$

For example:

$$\Delta T = \frac{F}{4\sigma T^3(1-g)\left[1 + \frac{1}{4\sigma T^3(1-g)}\frac{5}{4}\frac{\partial\alpha}{\partial T} - \frac{T}{4(1-g)}\frac{\partial g}{\partial T}\right]}$$

$\frac{\partial\alpha}{\partial T} < 0 \Rightarrow$ amplification

$\frac{\partial g}{\partial T} > \frac{4(1-g)}{T} \Rightarrow$ run away greenhouse effect.

Bony et al

$$\frac{dg}{d\,SST}$$

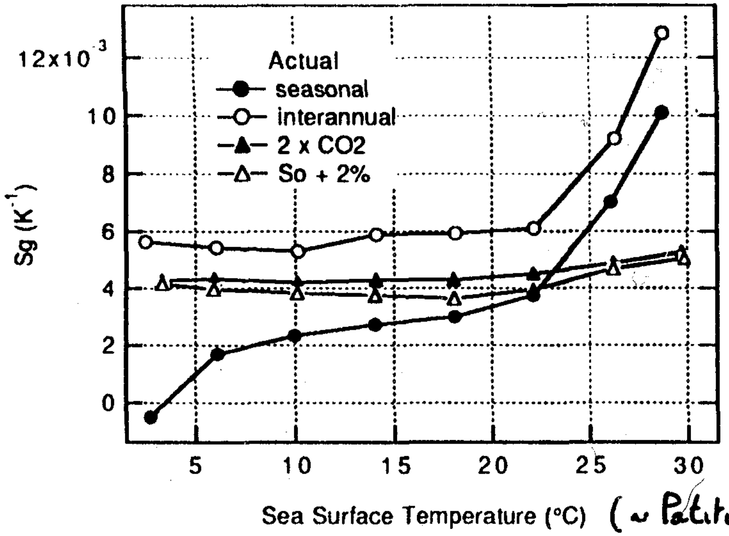

(~ latitude)

GLOBAL FIGURE

Derivative of clear-sky greenhouse index to SST (= "clear sky sensitivity")

(from off-line computations using the GCM)

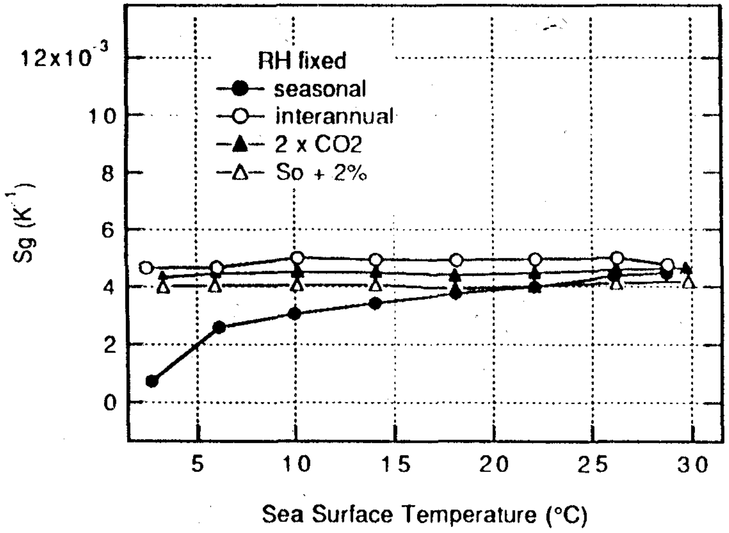

Relative Humidity fixed

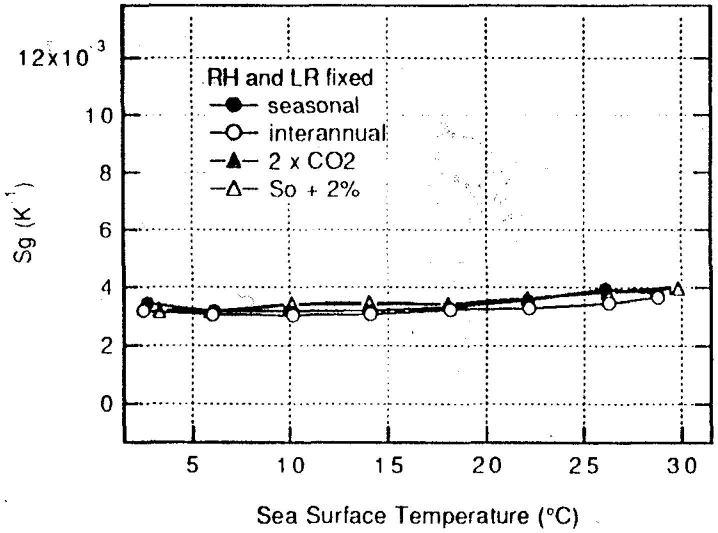

Relative Humidity and Lapse Rate Fixed

Observed and simulated sensitivity over the oceans

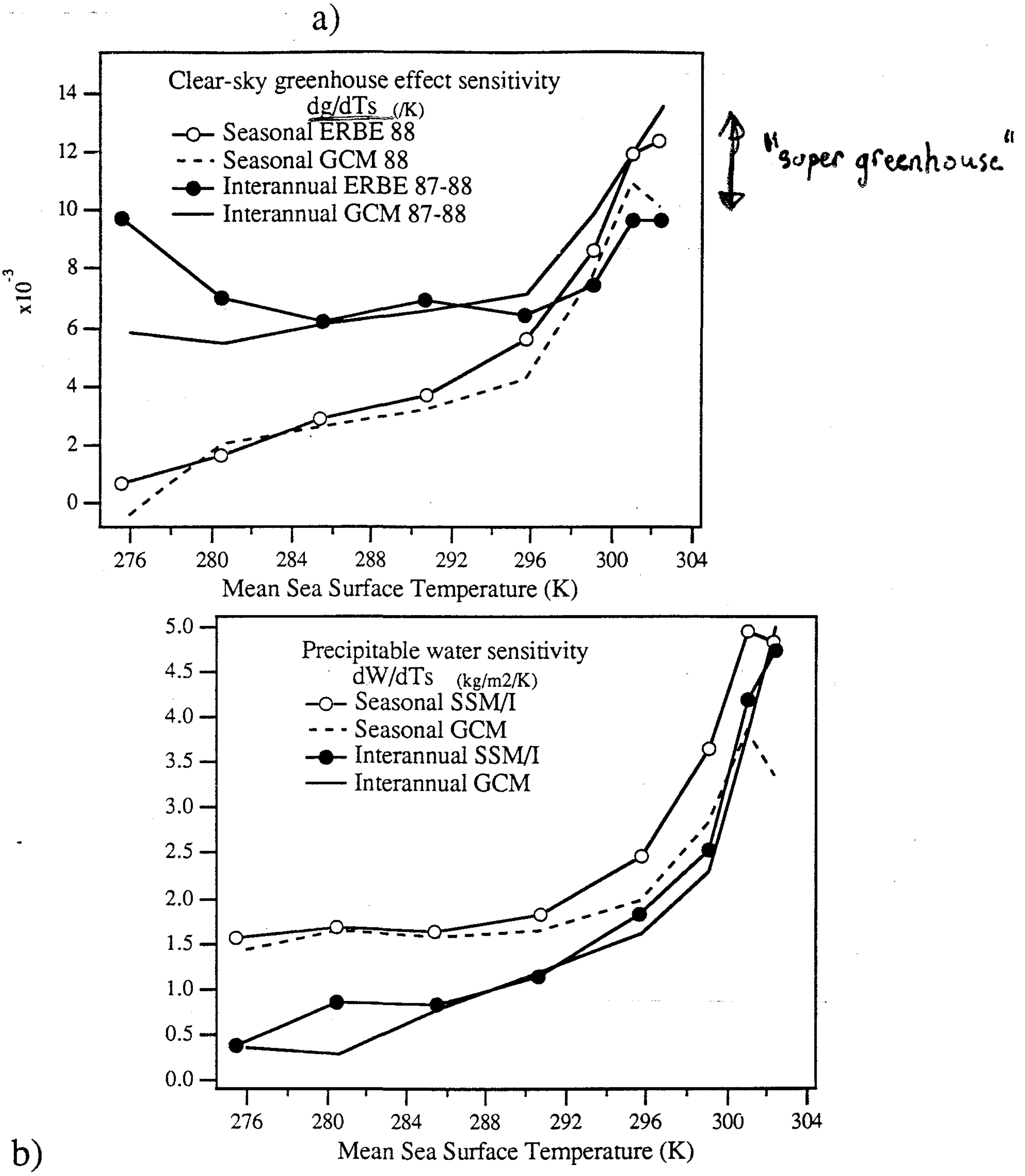

Seasonal and Interannual sensitivities over ocean of (a) the clear-sky greenhouse effect and of (b) the precipitable water, derived from satellite observations and from the LMD GCM.

prtub.aerod.co2275.moyan01an20- prtub.aeron.co2275.moyan11an20

A1

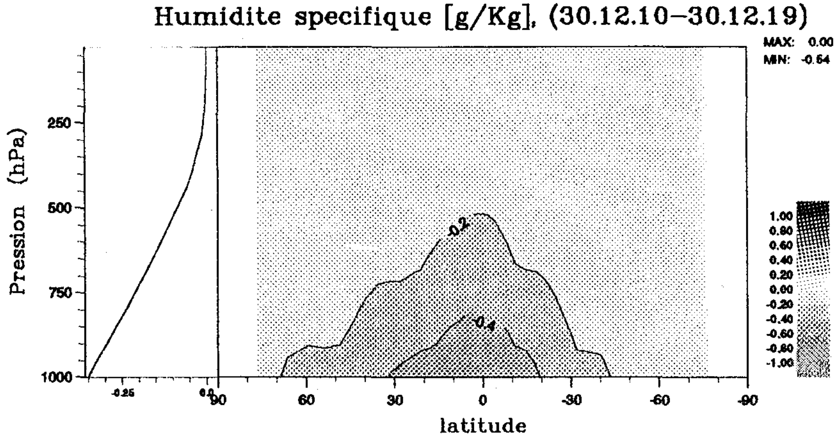
Humidite specifique [g/Kg], (30.12.10-30.12.19)

prtub.aeroa.co2275.moyan11an20- prtub.aeron.co2275.moyan11an2 LMD

A2

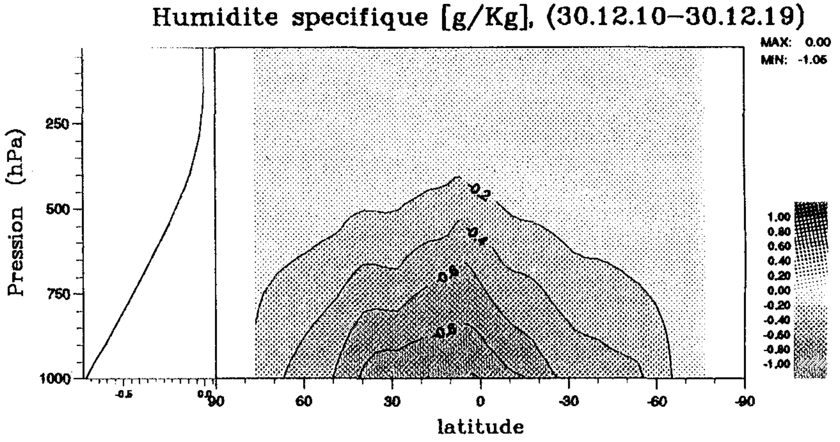
Humidite specifique [g/Kg], (30.12.10-30.12.19)

prtub.aeron.co2345.moyan11an20- prtub.aeron.co2275.moyan11an20

CO₂

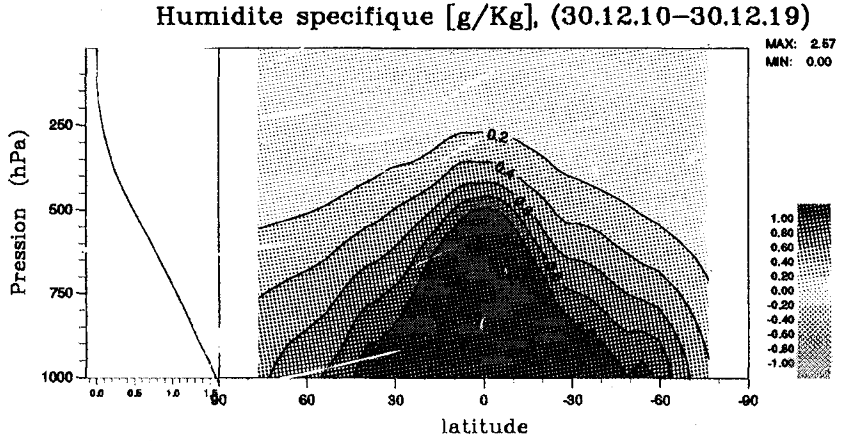
Humidite specifique [g/Kg], (30.12.10-30.12.19)

prtub.aeroa.co2345.moyan11an20- prtub.aeron.co2275.moyan11an20

T

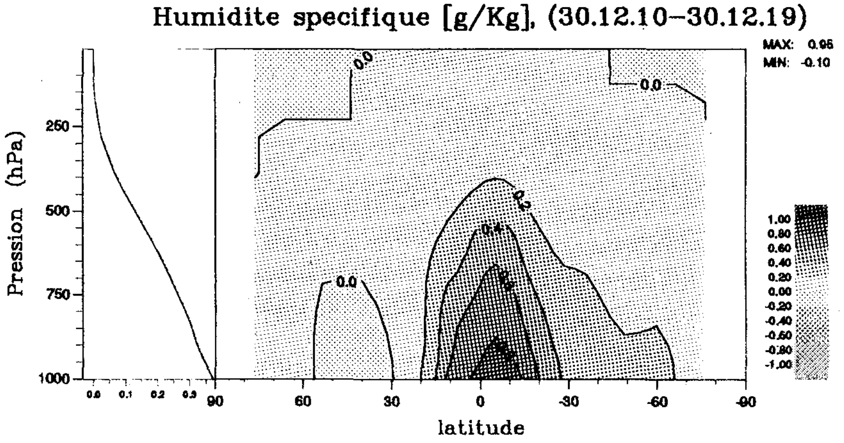
Humidite specifique [g/Kg], (30.12.10-30.12.19)

Water vapour and cloud feedbacks

→ importance of the vertical stratification

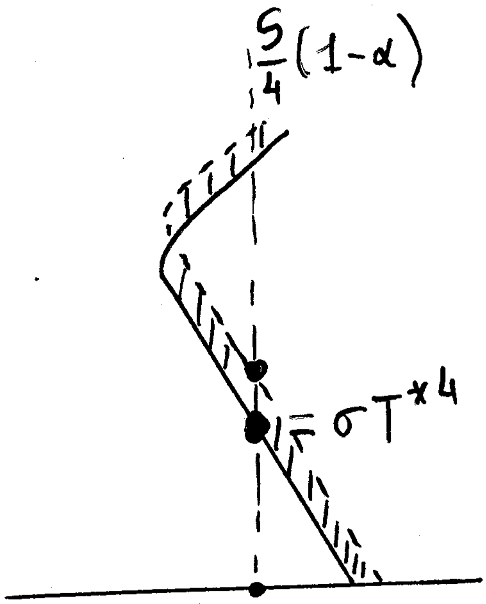

T^* = equivalent emission temperature

surface warms → because the emission level is higher, and the decreasing temperature gradient is imposed.

Geographical changes, seasonal changes, interannual changes and response to a global forcing ARE NOT EQUIVALENT.

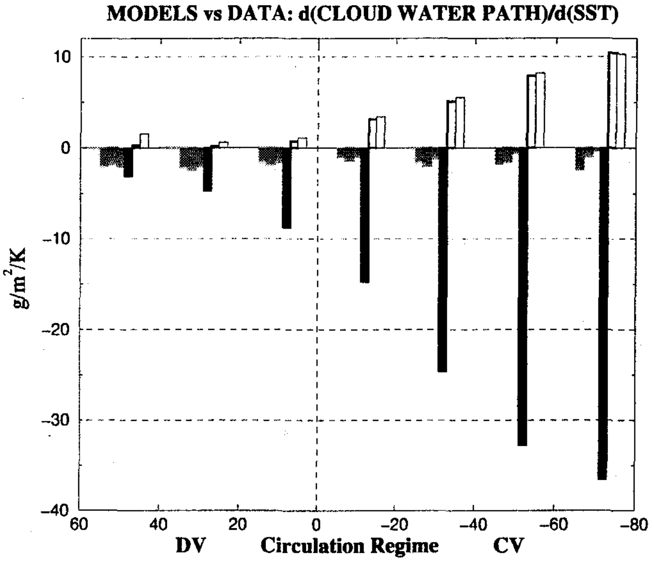

Figure 10: Sensitivity of the cloud liquid water path to SST changes derived from observations (black and white bars) and from the UKMO (filled bar), ECMWF (thick bar) and LMD (thin bar) models.

Han et al (GISS)

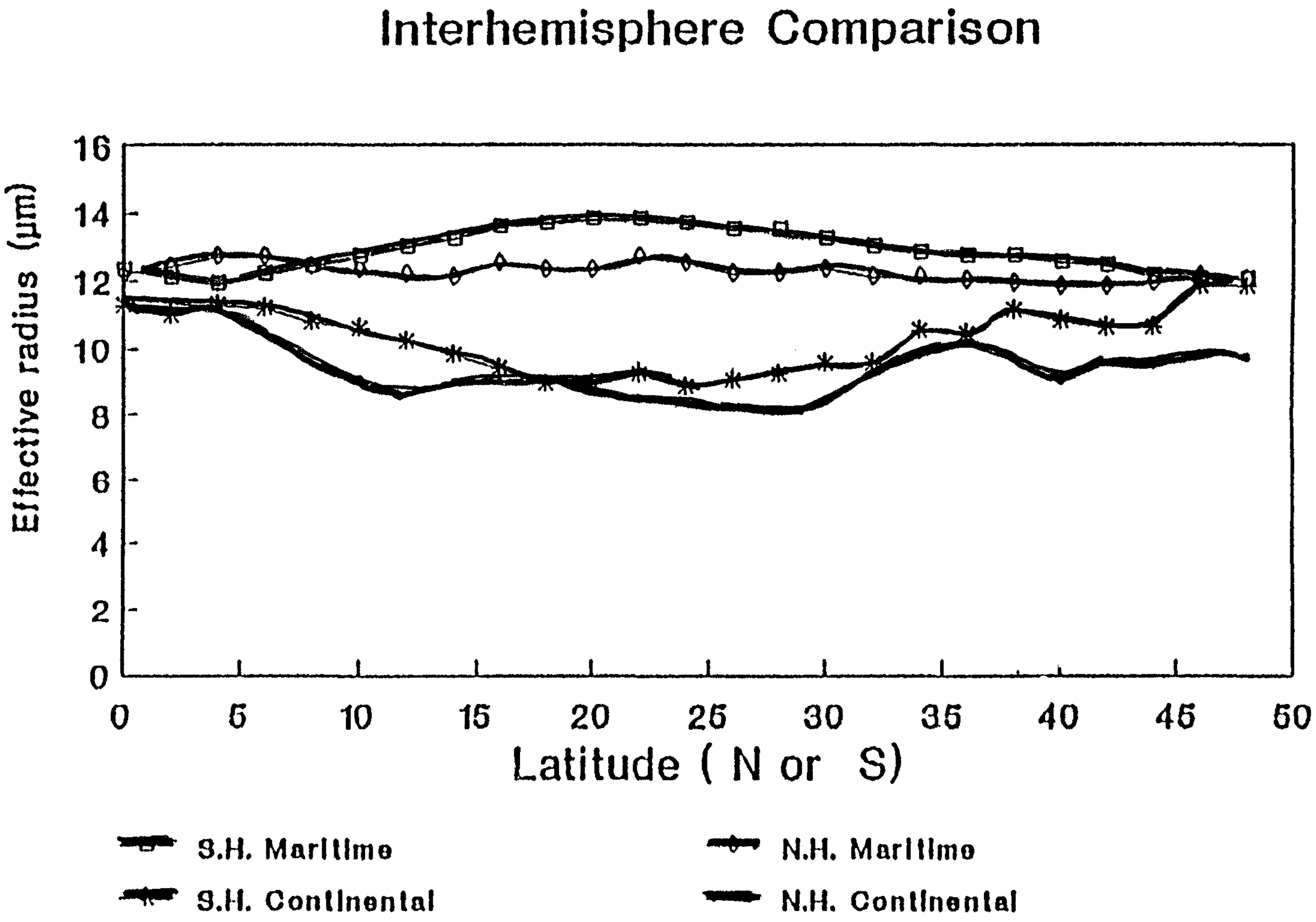

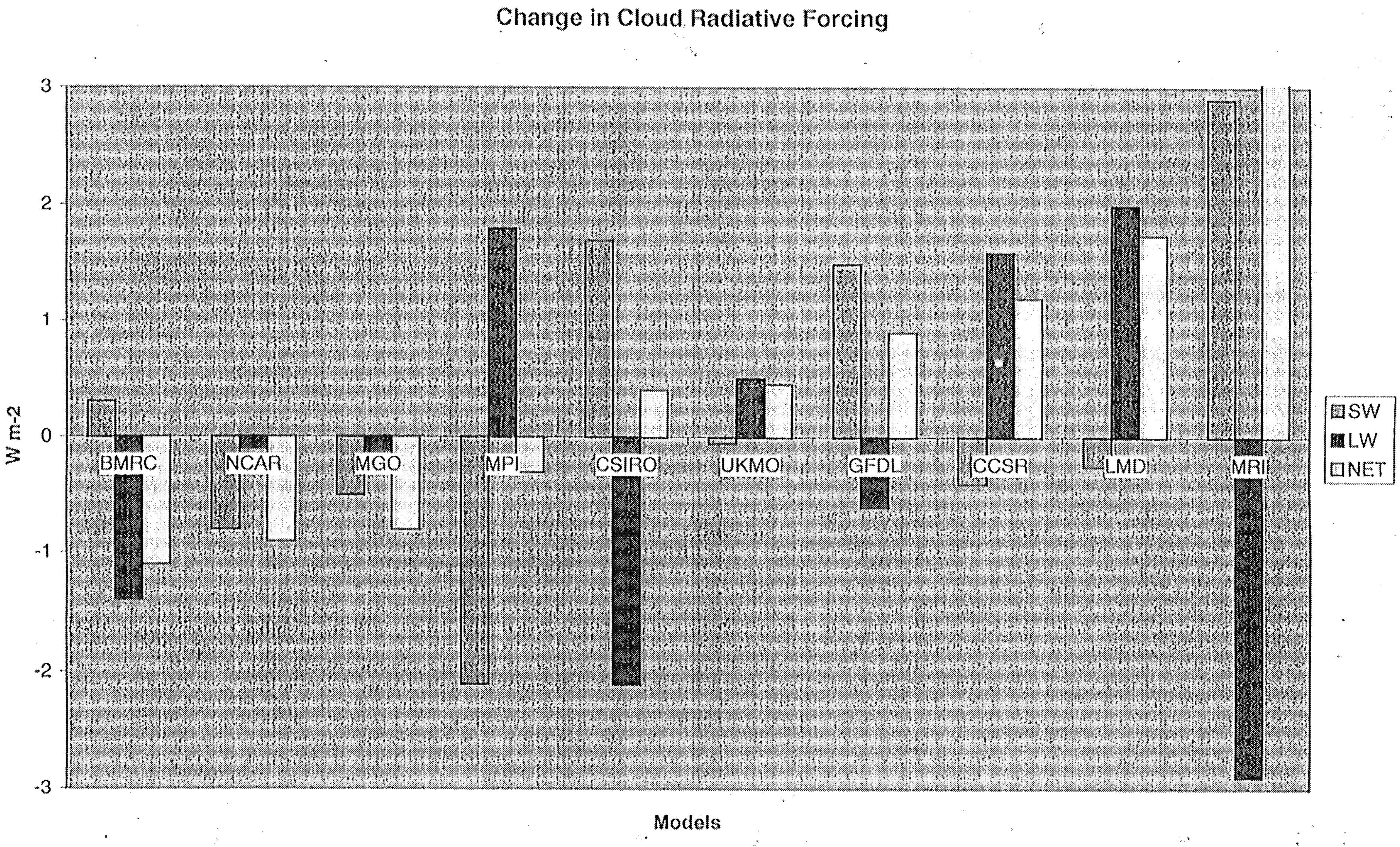
Change in Cloud Radiative Forcing
3
2
1
0
-1
-2
-3
W m-2
BMRC
NCAR
MGO
MPI
CSIRO
UKMO
GFDL
CCSR
LMD
MRI
Models
SW
LW
NET

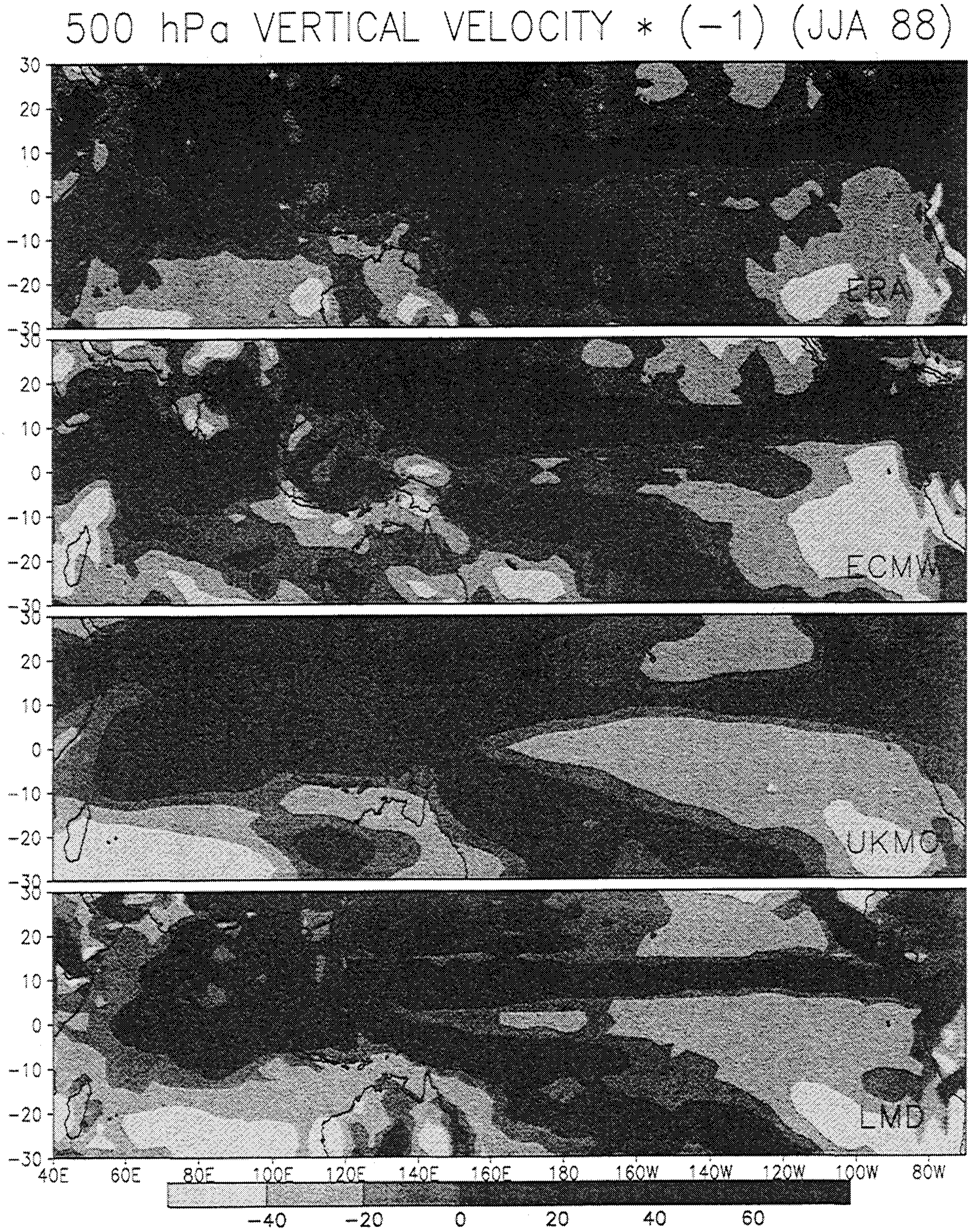

Figure 3: 500 hPa vertical velocity derived from NCEP re-analyses and simulated by the three models for June-July-August 1988. Units: hPa/day.

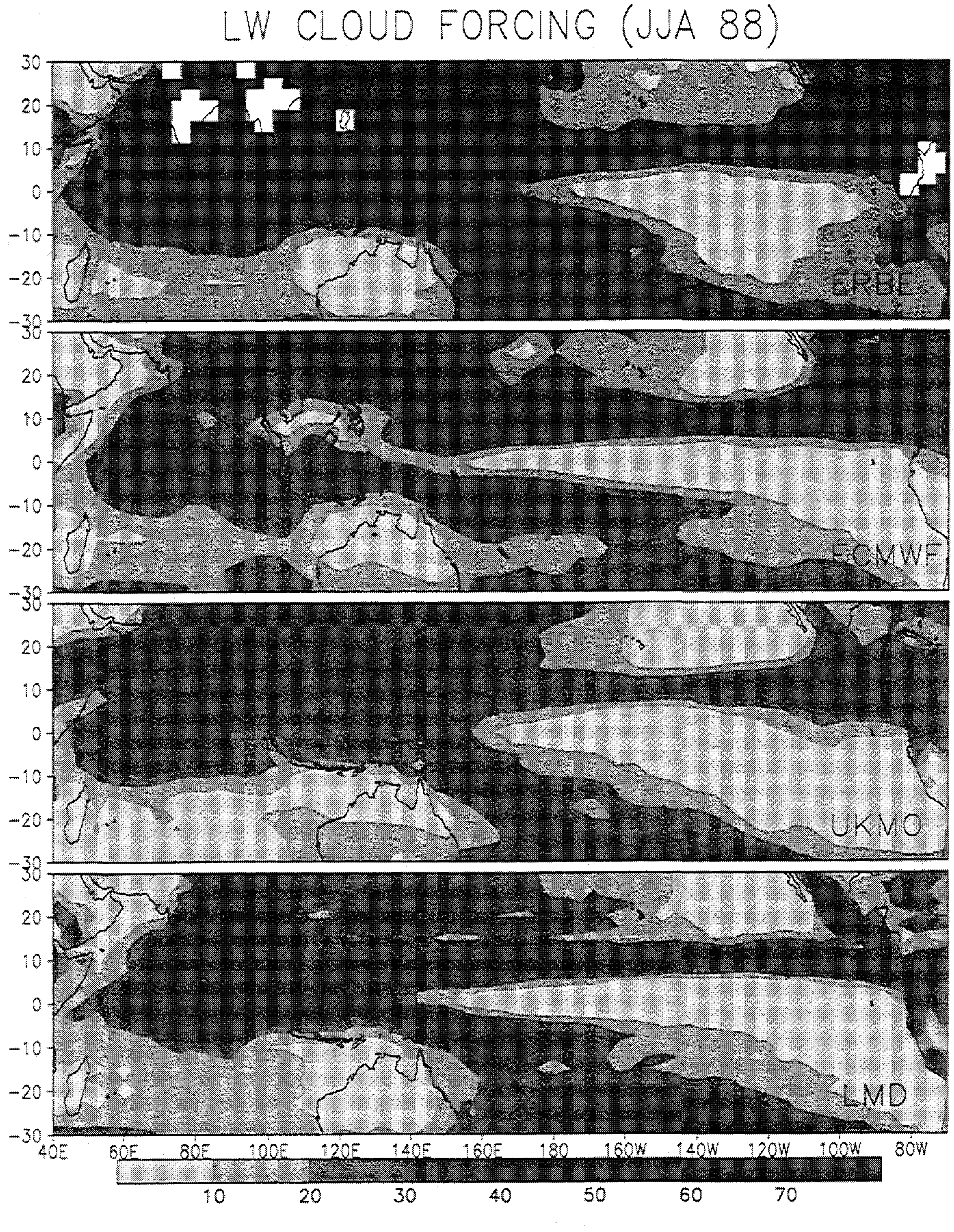

Figure 1: Longwave component of the cloud radiative forcing derived from ERBE data and simulated by the three models for June-July-August 1988. Units: W/m^2.

Bony, Sud, Lau
J. Climate.

Bony et al, 97

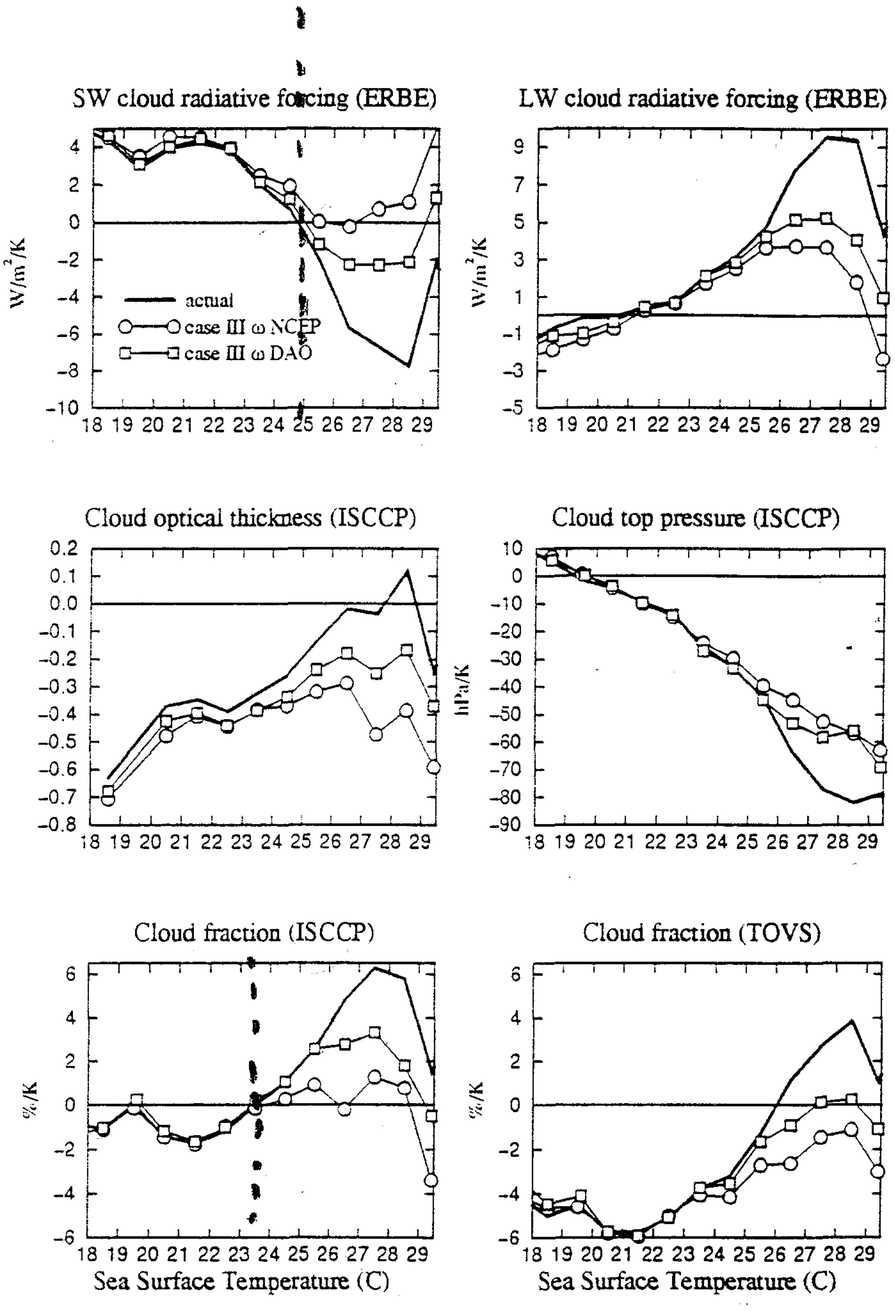

(Interannual variations)

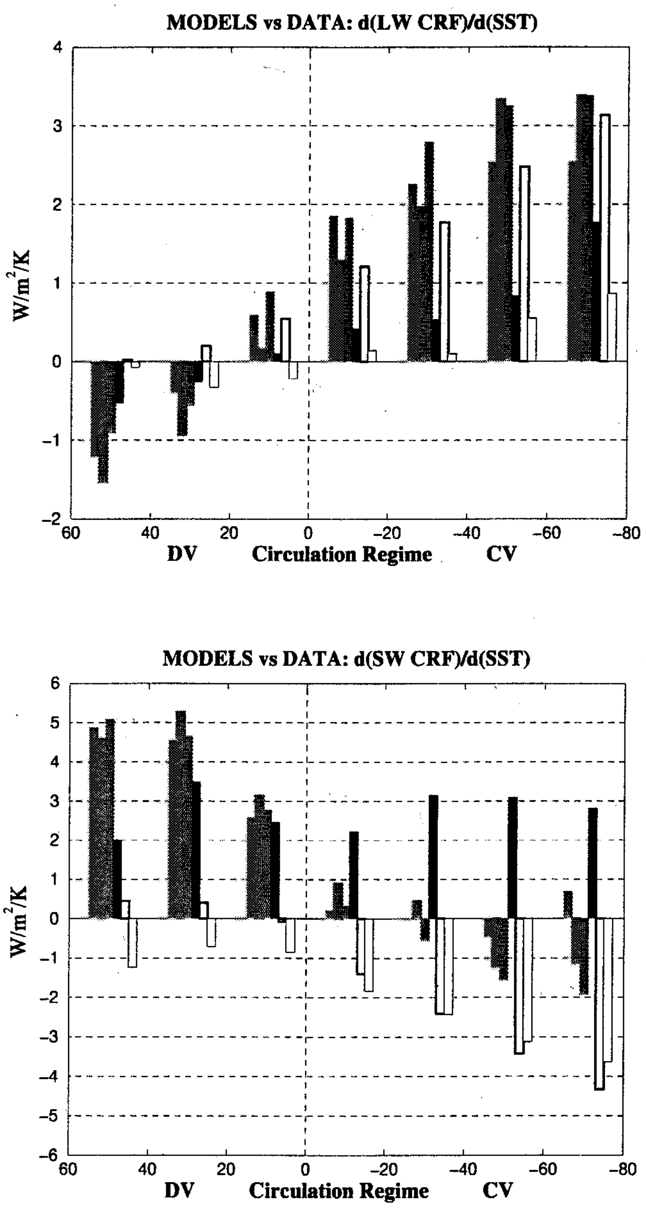

Figure 7: Sensitivity of the (top) LW CRF and (bottom) SW CRF to SST changes derived from data (grey bars) and from the UKMO (filled bar), ECMWF (thick bar) and LMD (thin bar) models.

Changement de nébulosité dû au forçage du CO_2

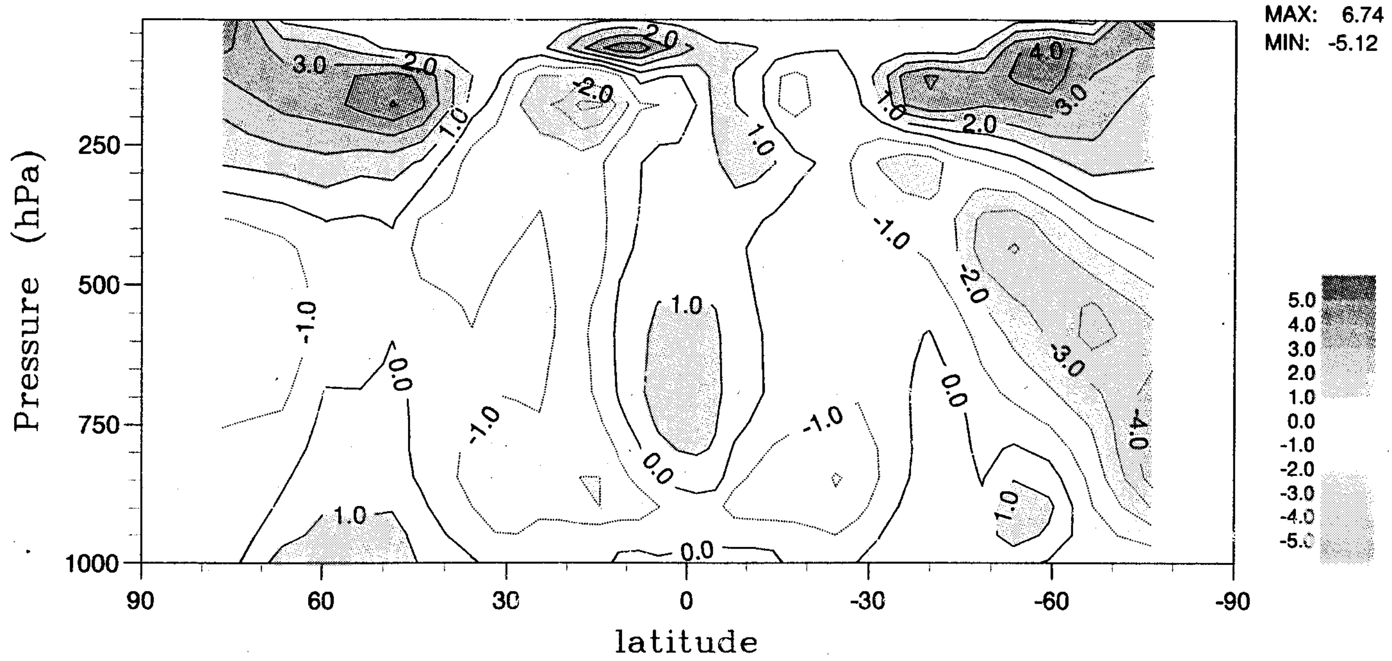

Changement de nébulosité dû au forçage des aérosols

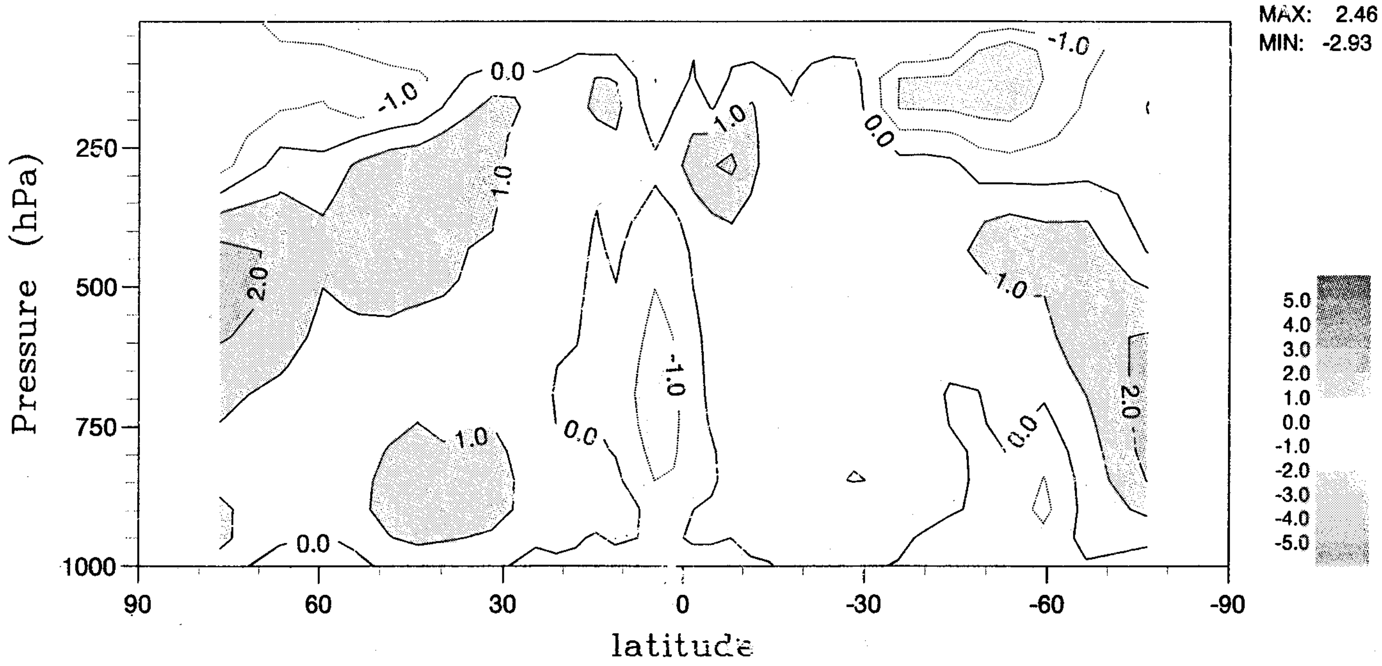

LMD

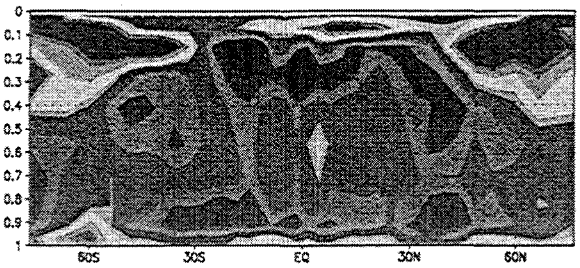

GrADS: COLA/IGES

CCM

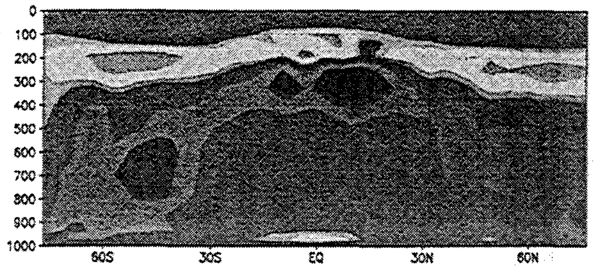

GrADS: COLA/IGES

Hadley

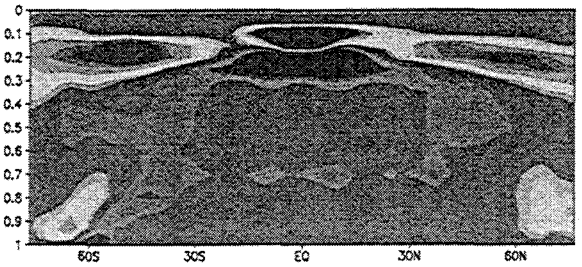

GrADS: COLA/IGES

GISS

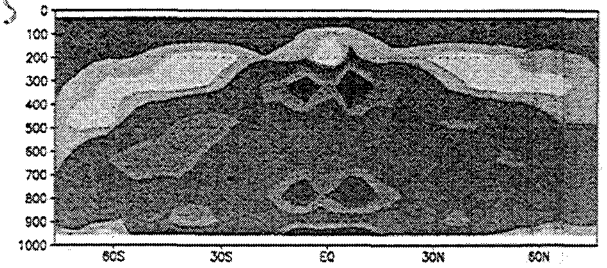

GrADS: COLA/IGES

BMRC

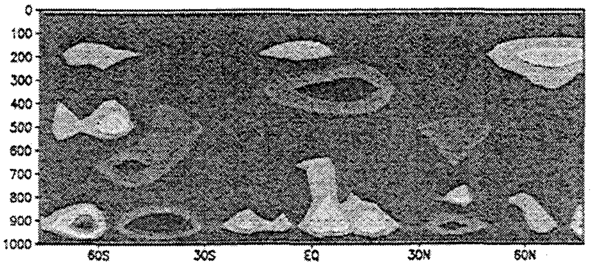

GrADS: COLA/IGES

MPI

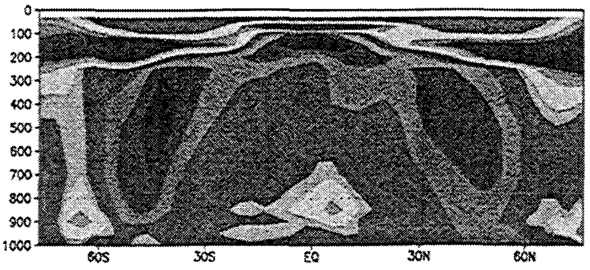

GrADS: COLA/IGES

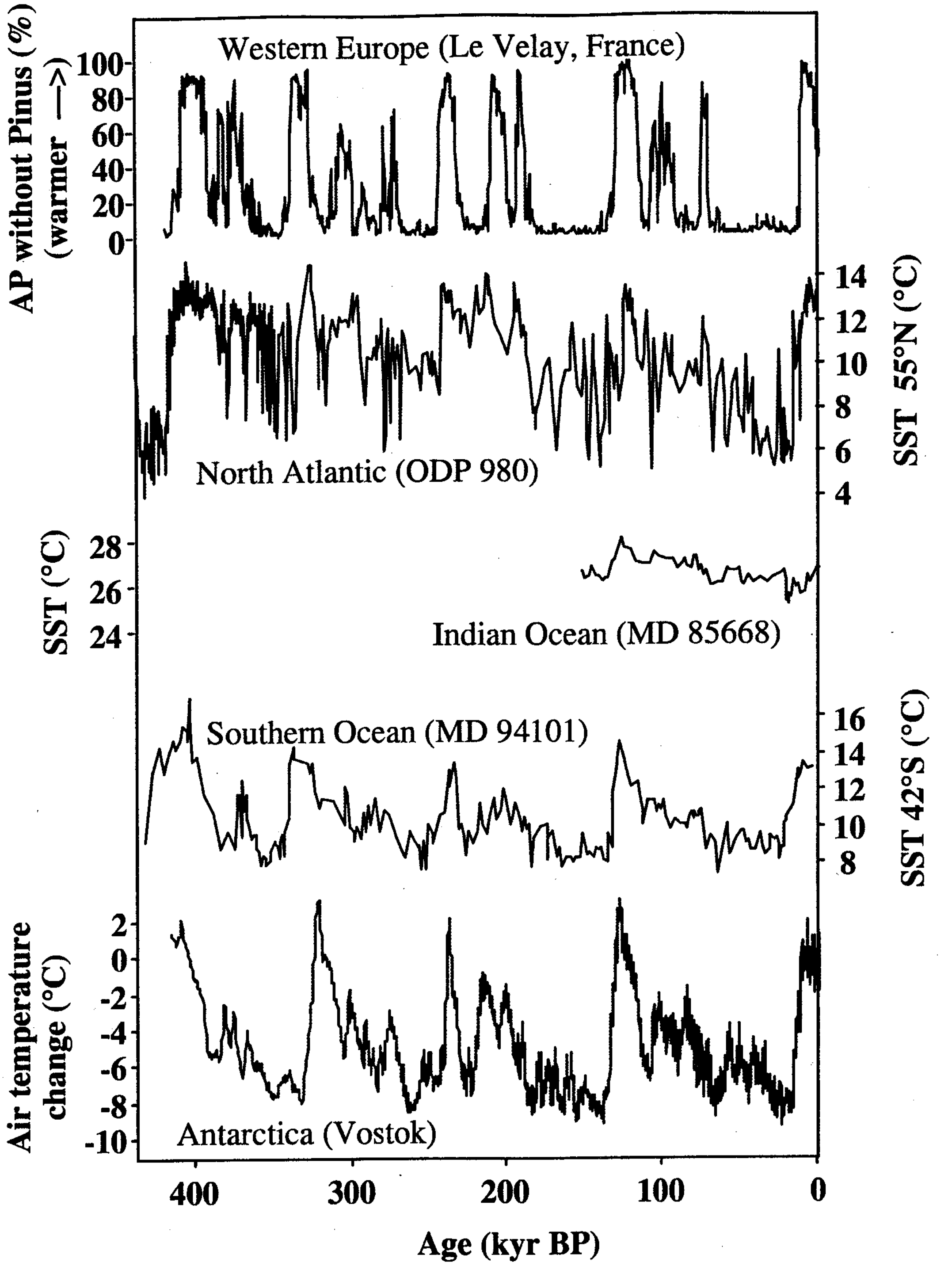

Nouvelle figure 4 cycles...

Première analyse spectrale d'une carotte sedimentaire oceanique (Hays, Imbrie and Schackleton, 76)

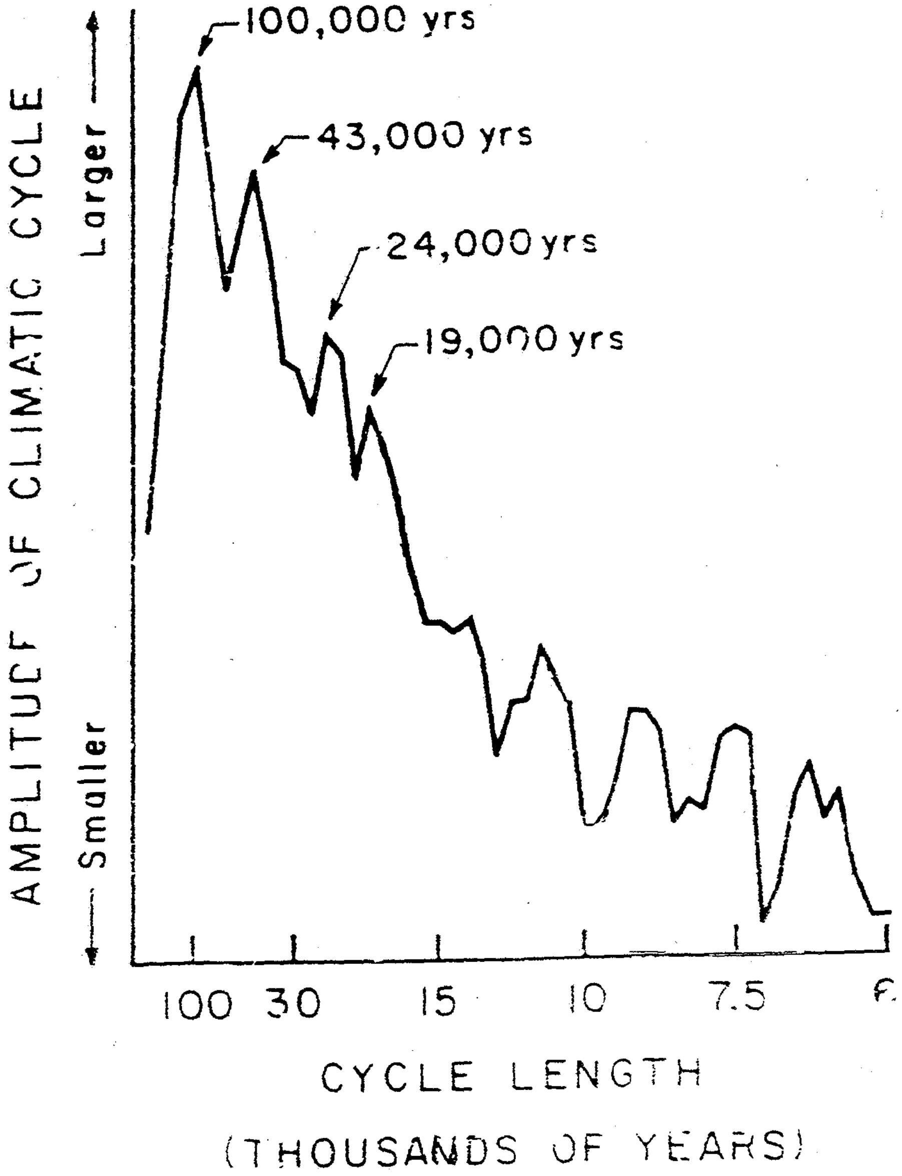

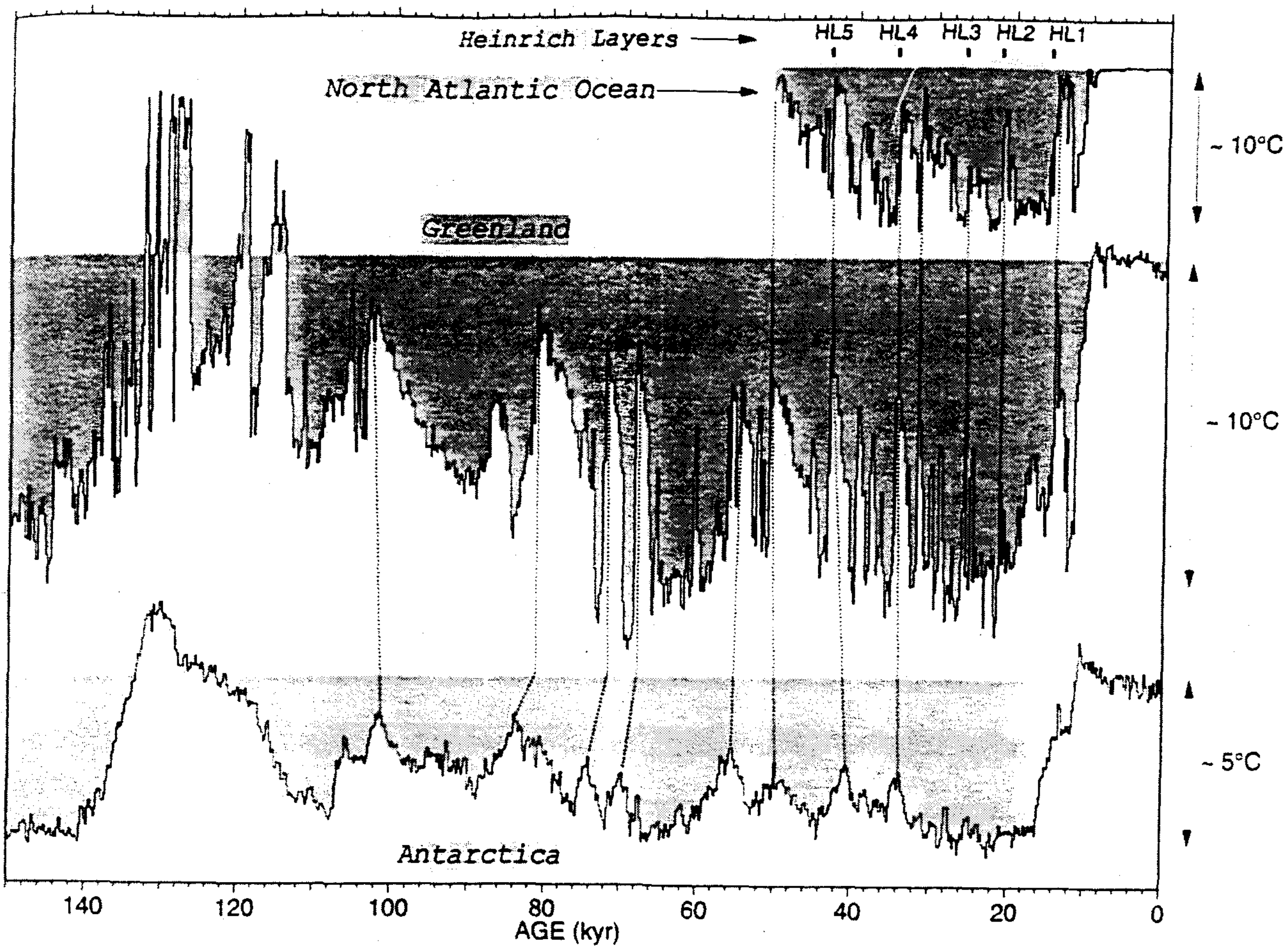

Figure 3.22: Reconstructed climate records showing rapid changes in the North Atlantic and in Greenland; the corresponding events (indicated by thin dashed vertical lines) are damped in the Antarctic record. Temperature changes are estimated from the isotopic content of ice (Greenland and Antarctica) and from faunal counts (North Atlantic). HL1 to HL5 indicate sedimentary "Heinrich" layers. Figure adapted from Jouzel et al. (1994).

temperature on century time-scales, over the past millennium, as less than ±0.5°C.

3.6.3 Rapid Cimate Changes in the Last 150,000 Years

The warming of the late 20th century appears to be rapid, when viewed in the context of the last millennium (see above, and Figures 3.20, 3.21). But have similar, rapid changes occurred in the past? That is, are such changes a part of the natural climate variability? Large and rapid climatic changes did occur during the last ice age and during the transition towards the present Holocene period which started about 10,000 years ago (Figure 3.22). Those changes may have occurred on the time-scale of a human life or less, at least in the North Atlantic where they are best documented. Many climate variables were affected: atmospheric temperature and circulation, precipitation patterns and hydrological cycle, temperature and circulation of the ocean.

Much information about rapid climatic changes has recently been obtained either from a refined interpretation of existing records or from new ice, ocean and continental records from various parts of the world. Of particular significance are those concerning the North Atlantic and adjacent continents such as the GRIP (Dansgaard *et al.*, 1993) and GISP 2 (Grootes *et al.*, 1993) central Greenland ice cores, numerous deep-sea core records from the North Atlantic, and continental records (lake sediments, pollen series, etc.) from Western Europe and North America. These records provide descriptions of the last glacial period and the following deglaciation. The observed rapid changes are often large in magnitude, and thus there is considerable confidence in their reality.

$$C_T \frac{dT}{dt} = R_S - R_T \qquad \frac{dR_S}{dV} < 0 \text{ (albedo)}$$

$$C_V \frac{dV}{dt} = \text{Accumulation} - \text{Melting} \qquad \frac{dAcc}{dT} > 0$$

↑
volume
of ice

$C_T \neq Ce$

⇓

oscillations

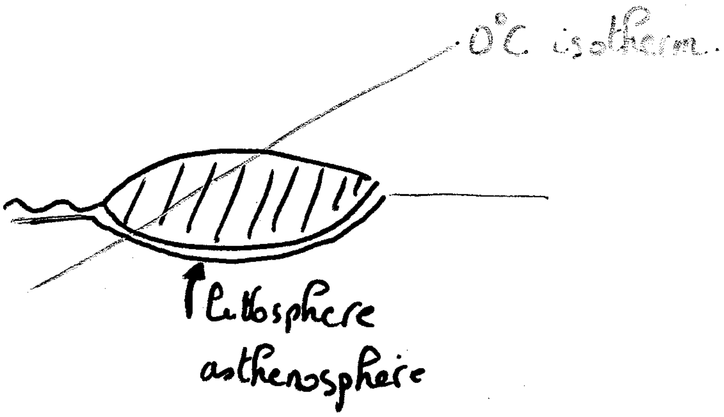

Other components:

- asthenosphere delayed response
- geothermal heating of ice base
- greenhouse gases amplification

- - - - - - -

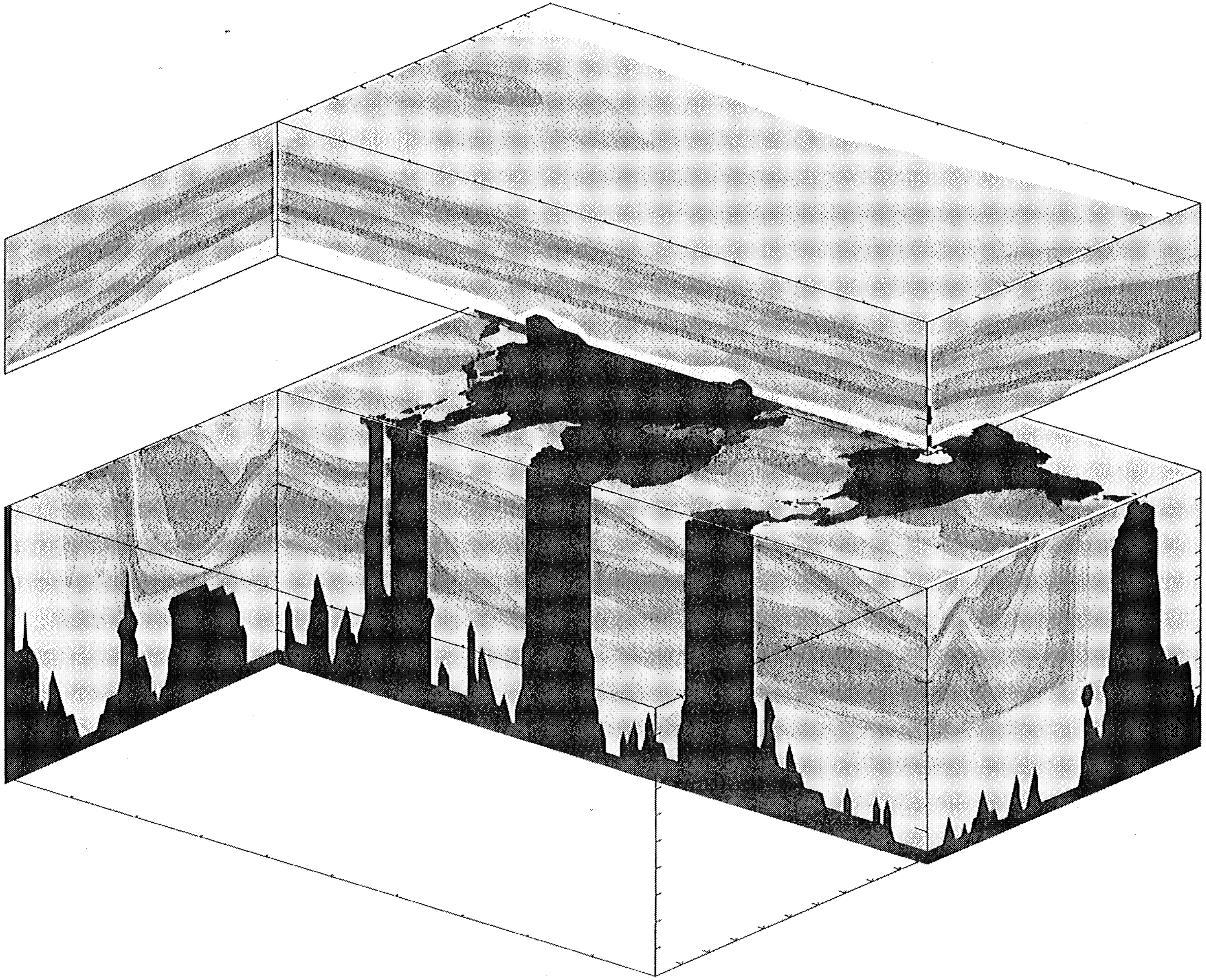

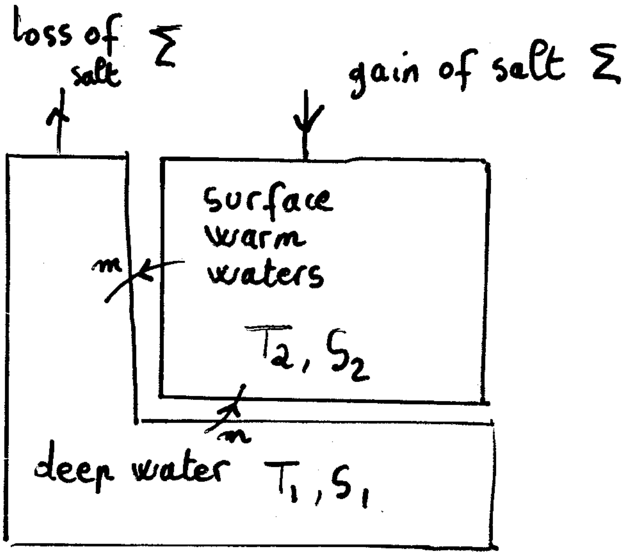

$$m = \mu \Delta \rho = -\mu \alpha (T_1 - T_2) + \mu \beta (S_1 - S_2)$$

$$= \mu \alpha \Delta T - \mu \beta \Delta S$$

$$\frac{dS_1}{dt} = -\Sigma + |m| \Delta S$$

$$\frac{dS_2}{dt} = \Sigma - |m| \Delta S$$

$$\frac{1}{2} \frac{d}{dt} \left(x \right) = \frac{\Sigma}{(\alpha \Delta T)^2 \mu} - \left| 1 - x \right| x = 0$$

$$x = \frac{\beta \Delta S}{\alpha \Delta T}$$

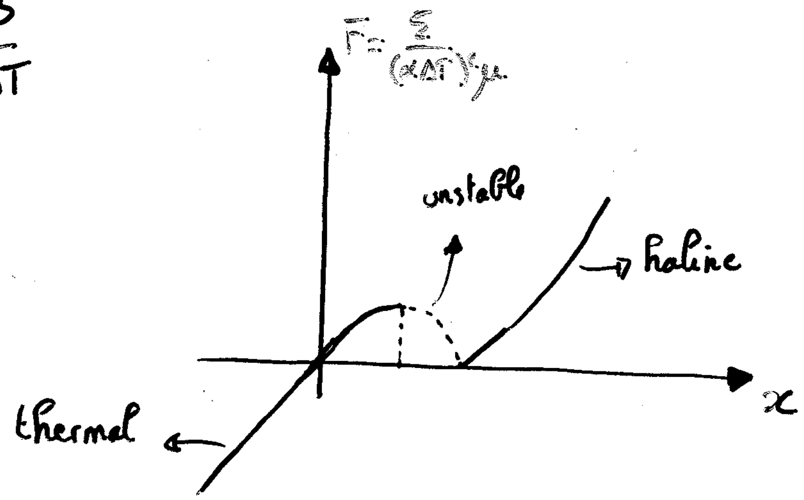

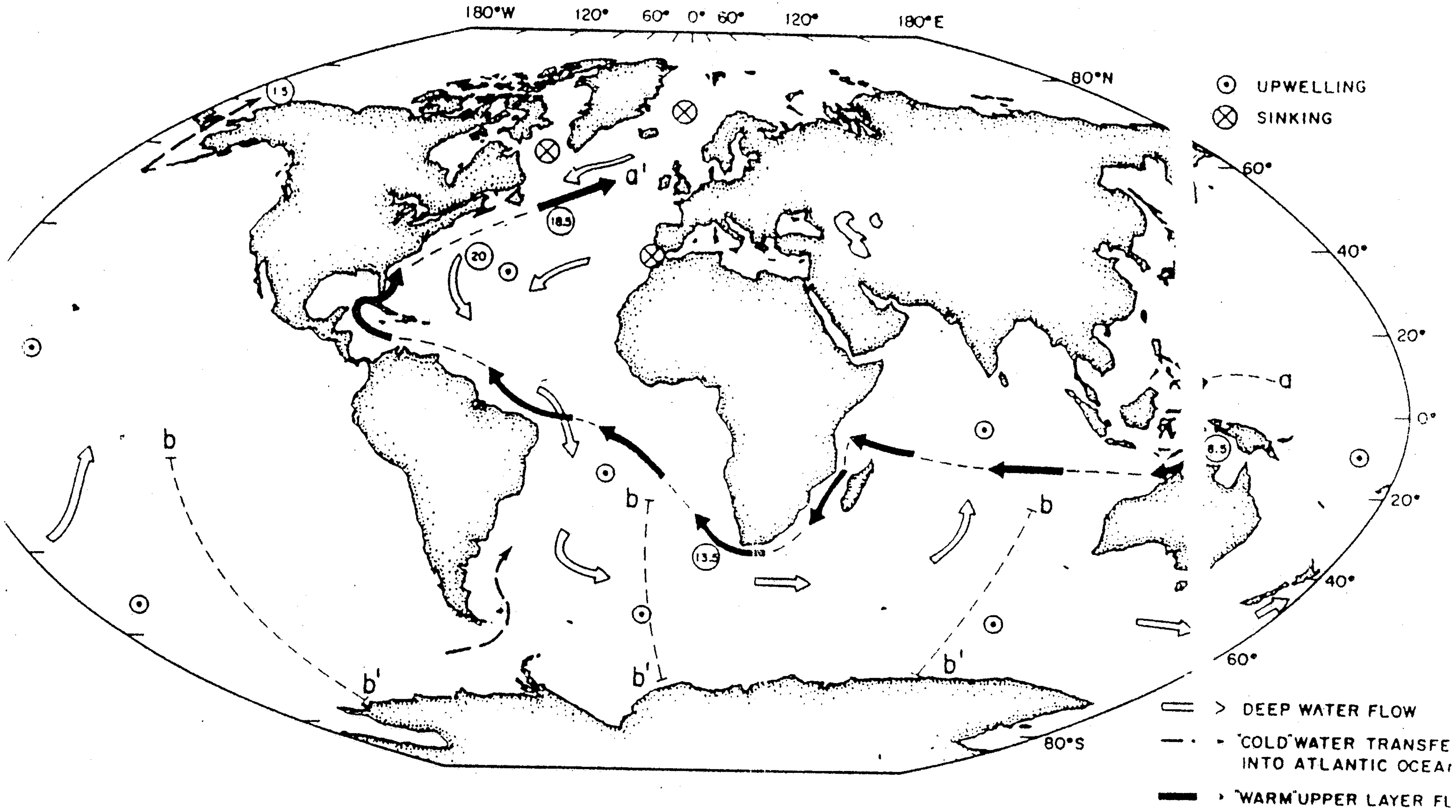

Fig. 10. A schematic of the interocean exchanges of thermocline waters and of deep waters, as inferred b *Gordon* [1986].

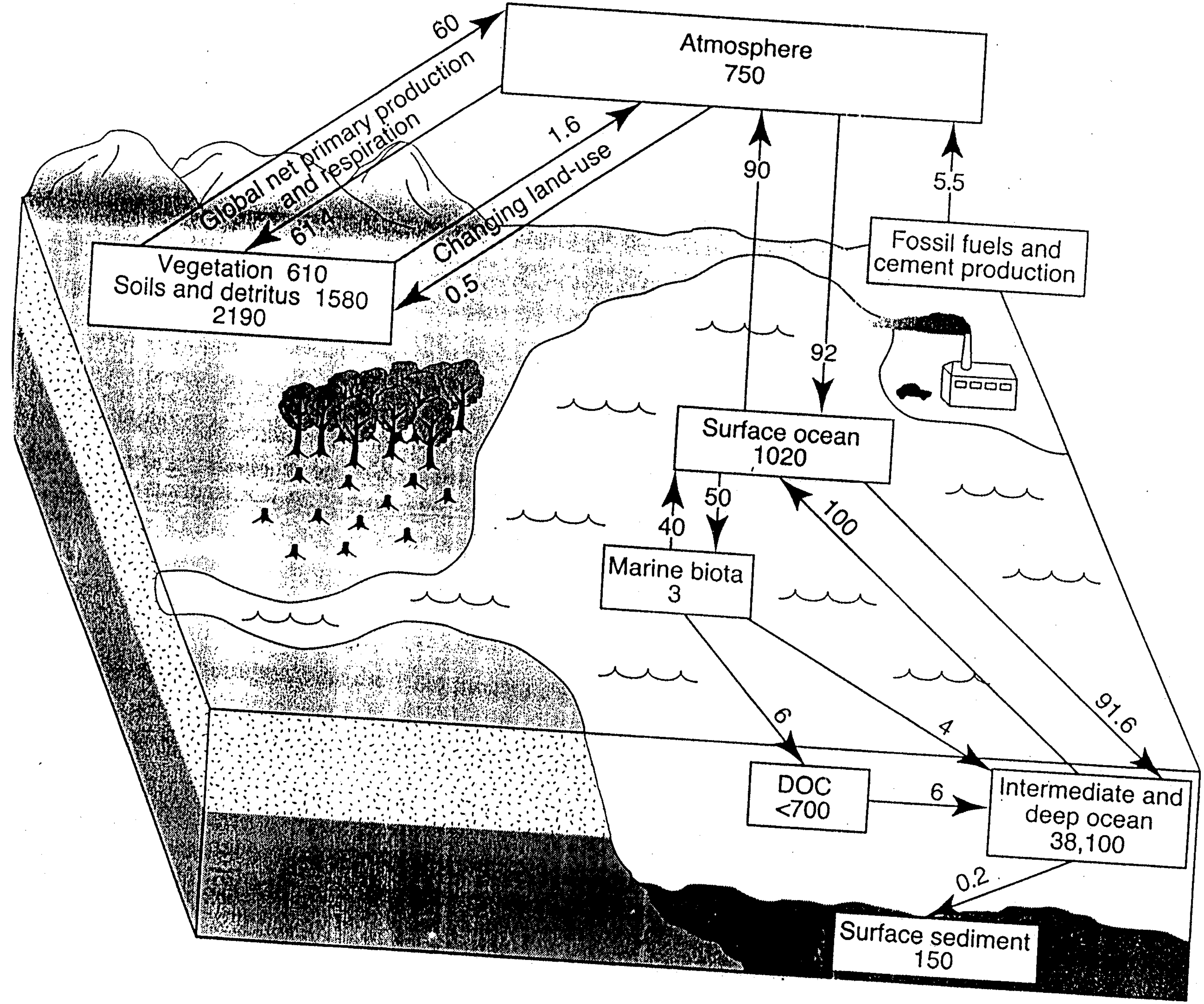
Atmosphere
750
60
Global net primary production
and respiration
61.4
1.6
Changing land-use
0.5
Vegetation 610
Soils and detritus 1580
2190
90
92
5.5
Fossil fuels and
cement production
Surface ocean
1020
40
50
100
Marine biota
3
6
4
91.6
DOC
<700
6
Intermediate and
deep ocean
38,100
0.2
Surface sediment
150

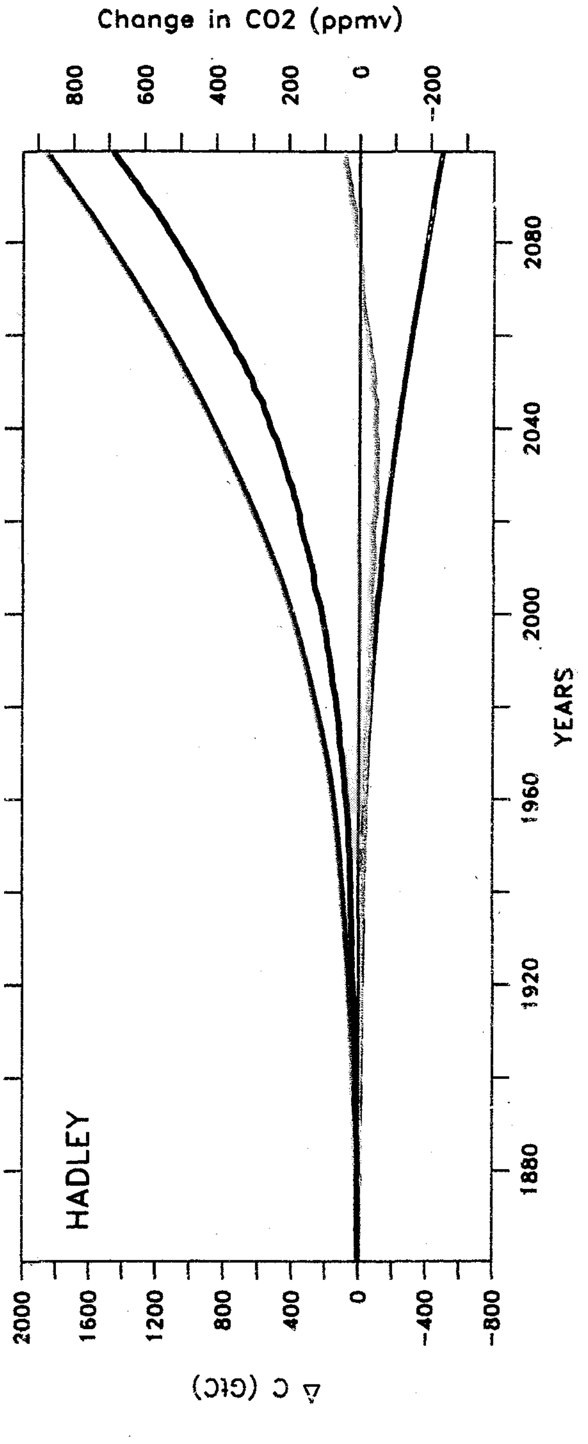HADLEY
Change in CO2 (ppmv)
800
600
400
200
0
-200
2000
1600
1200
800
400
0
-400
-800
Δ C (GtC)
1880
1920
1960
2000
2040
2080
YEARS

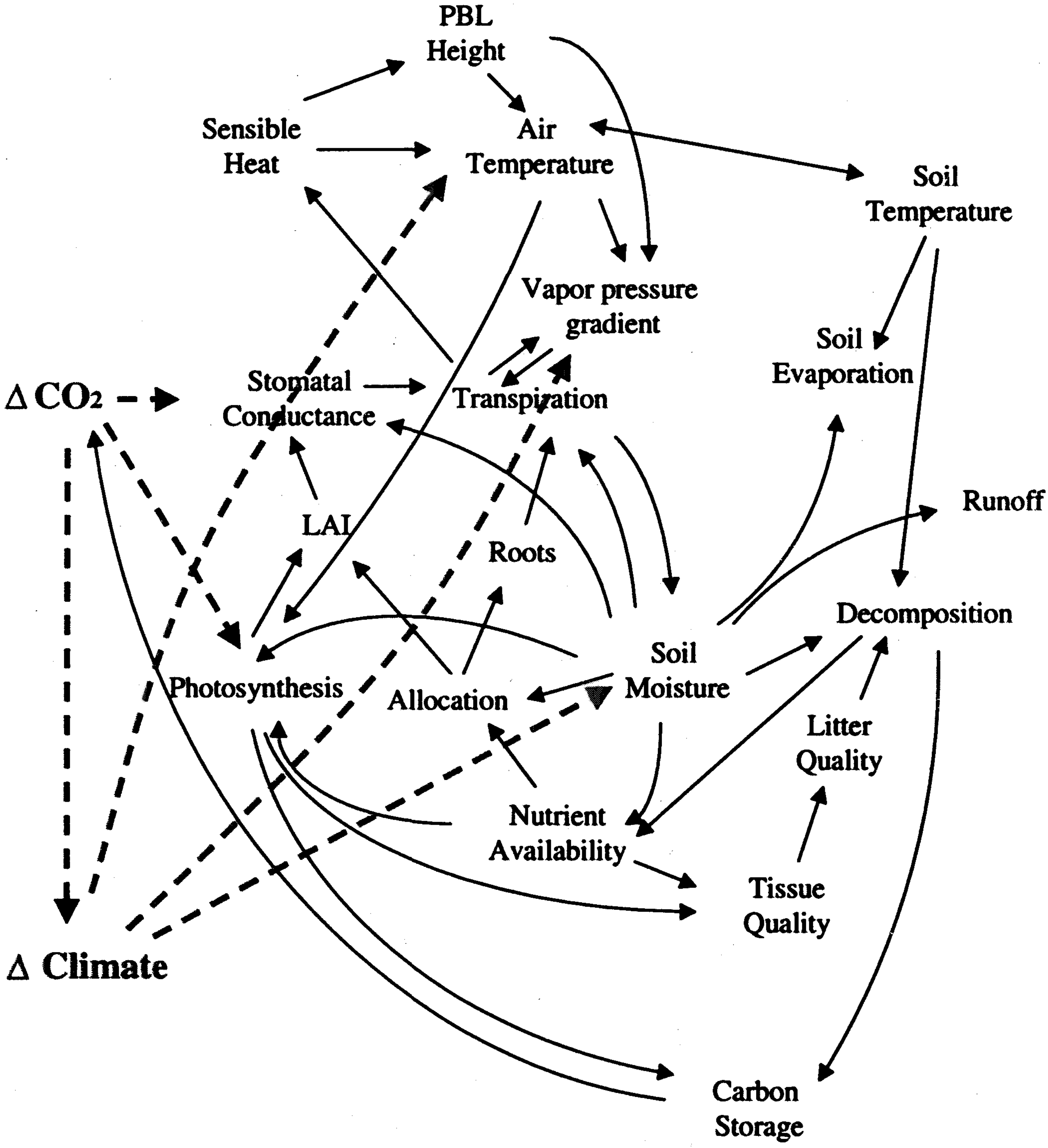
PBL
Height
Sensible
Heat
Air
Temperature
Soil
Temperature
Vapor pressure
gradient
Soil
Evaporation
Δ CO2
Stomatal
Conductance
Transpiration
Runoff
LAI
Roots
Decomposition
Soil
Moisture
Photosynthesis
Allocation
Litter
Quality
Nutrient
Availability
Tissue
Quality
Δ Climate
Carbon
Storage

View of atmospheric response:

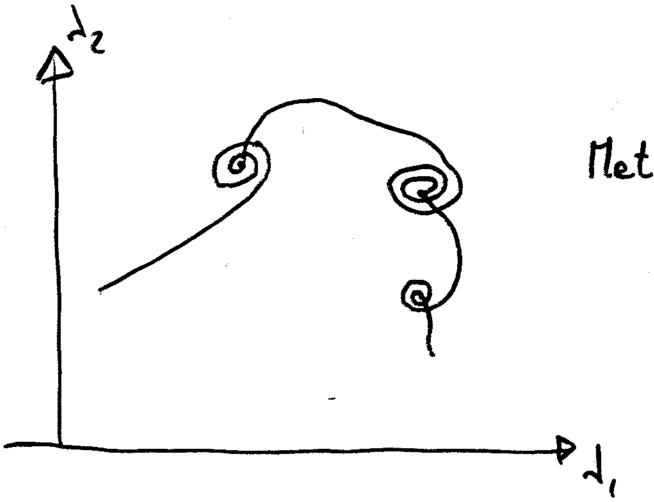

Meta-stable "Modes"

The population of the modes may change more than the modes themselves.

Oscillation Nord Atlantique (NAO)

la SLP

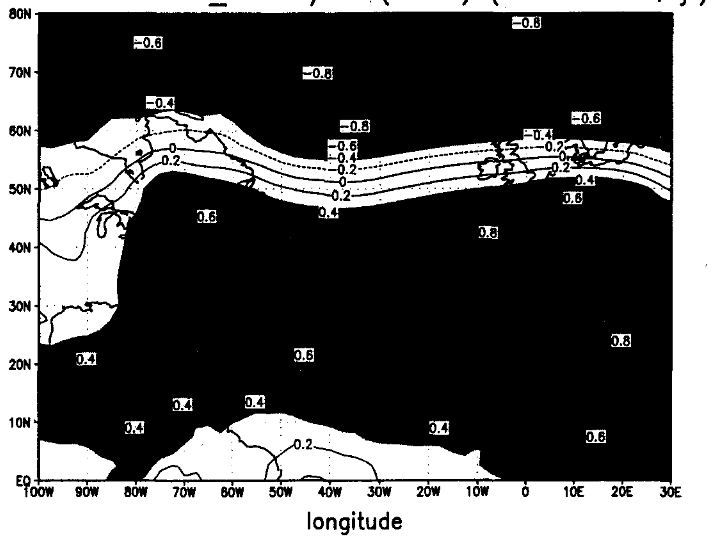

Correlation NAO_hurrell/SLP(NCEP) (1958–1995,djf)

la SST

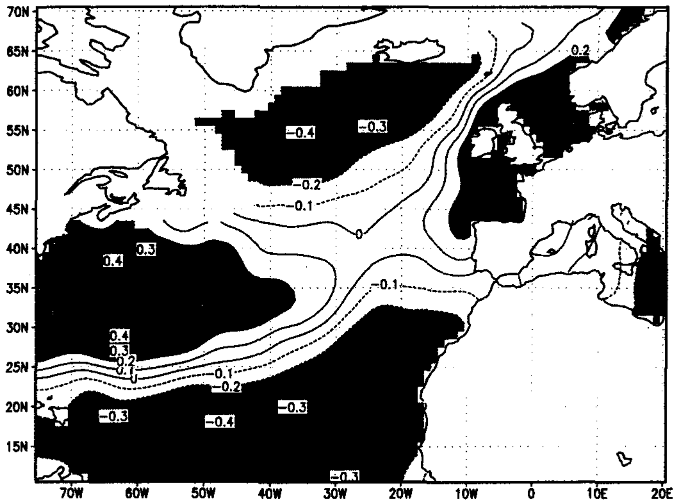

Correlation GISST/NAO Hurrell (1903–1992,jfm)

Bjerknes (1964), Cayan (1992), Kushnir (1994), Grötzner et al. (1998)

$$Indice_{NAO} = (\frac{slp_A(t) - \overline{slp_A}}{\sigma_A}) - (\frac{slp_I(t) - \overline{slp_I}}{\sigma_I})$$

Hurrell (1995), Hurrell et van Loon (1997)

indice NAO 1864–1995 Hurrell (Dec–Mars)